Student thesis series INES nr 439

Urban flood modelling: a GIS based approach in Lomma, Skåne region

Michael Araya Ghebremariam

2017
Department of Physical Geography and Ecosystem Science
Lund University
Sölvegatan 12
S-223 62 Lund
Sweden

Michael Araya Ghebremariam (2017) **Urban flood modelling: a GIS based approach in Lomma, Skåne region**

Master degree thesis, 30 credits in Physical Geography and Ecosystem Analysis
Department of Physical Geography and Ecosystem Science, Lund University
Level: Master of Science (MSc)
Course duration: *January* 2015 until *January* 2017

Disclaimer

Urban flood modelling: a GIS based approach in Lomma, Skåne region

Michael Araya Ghebremariam

Master thesis, 30 credits, Physical Geography and Ecosystem Analysis

Supervisor: Andreas Persson

Senior lecturer at Department of Physical Geography and Ecosystem Science

Abstract

Land use changes related to urbanization replaces pervious land surfaces with impervious surfaces which have less capacity to infiltrate and store water into the ground. Impervious surfaces reduce infiltration and increase surface runoff from the catchment, causing flooding to occur. Recently, GIS-based distributed hydrological models have been commonly used to perform a detailed analysis and modelling of flooding in urban areas. However, the implementation of these models require high level proficiency in GIS and hydrology. Moreover, this approach is generally beyond municipalities budget in cost and time. In this study a GIS-based model that can perform urban flood modelling is developed. In the DEM pre-processing step, integration of spatial data is done using Arc Hydro tools. Calculation of flow accumulation from the catchment is performed using two flow routing algorithms (1) the deterministic eight-node algorithm (D8) and (2) the Triangular Form Based Multiple Flow algorithm (TFM). D8 algorithm assumes that flow at a point follows only the steepest downhill slope to one of the eight possible directions. TFM algorithm on the other hand estimates flow distribution values proportionally to the slope gradient in each direction. The effect of street inlet's flow interception capacity is introduced into the analysis through preparing a weight raster and running flow accumulation with weight. In D8 method, this is done by first delineating sub-watershed areas that contribute flow to each street inlets, then assign weight value to all cells that belong to a sub-catchment. In TFM method on the other hand, volume of flow which is equal to the flow interception capacity of street inlets is directly reduced from the flow accumulation at sink cells representing the inlets. The results of this study show that flow accumulation before the inclusion of street inlets interception effect in the analysis is **57,271 m^3** and **45,028 m^3** using D8 and TFM methods respectively. After street inlets interception effect is included in the analysis however, the results show that weighted flow accumulation is reduced to **33,316 m^3** and **10,893 m^3** using D8 and TFM methods respectively. In addition, **202** flooding incidents at sink cells are identified using D8 method, this number drops to **80** sink cell using TFM method.

Acknowledgements

First, I would like to thank my supervisor, Andreas Persson for his continuous assistance and encouragement throughout the research period. I would also like to thank the municipality of Lomma for providing us with the data without which this paper would not have been successful. Thanks also to Joel Ochieng for his support in editing the paper.

Table of Contents

List of Figures

List of Tables

Abbreviations

DEM	Digital elevation model
GIS	Geographical information systems
D8	Deterministic eight-node algorithm
TFM	Triangular form based multiple flow algorithm
SFD	Single flow direction algorithm
MFD	Multiple flow direction algorithm

1. Introduction

Floods are common natural hazards all over the world. Floods cause extensive damage to properties and loss of life in flood prone areas as well. According to (Dilley, et al., 2005) flood prone areas cover a third of the world's land area and 82% of the population. Floods can also cause serious difficulties to the stable fabric of a community (Ghosh, 2014) through damaging land developed for housing or agriculture, as well as roads and infrastructure. In addition, flood waters can cause large scale erosion of land by creating high runoff from catchment areas, as well as damage to drainage channels, bridge abutment, sewer outfall and other structures (Ghosh, 2014).

Some trends such as urbanization and industrial activities can increase the risk of flooding in areas that are flood plains of hydrological watersheds. Therefore, according to (Aksoy, et al., 2016) it is important to define clearly the flood prone areas in advance, in order to put in place adequate preventive measures that will minimize any damage the flood may cause. Digital terrain models (DEMs) can be used to determine watershed boundaries, drainage patterns and simplified flow calculations in rural areas (Beven & Moore, 1993). However, in urban areas, similar analysis is complicated by the fact that there are 2 different terrains to be considered (1) the original terrain shape and its natural drainage pattern as well as (2) the constructed terrain of streets and buildings which cause changes in the direction of drainage path (Beven & Moore, 1993). Alternatively, accurate estimation of overland flow distribution in urban environment can be achieved by integrating spatial data such as street inlets and building with DEM using Arc Hydro tools. Arc Hydro tools is a data model and toolset which can be used for integrating geospatial and temporal water resource information and processing it within ESRI's ArcGIS geographic information system (Maidment, 2004). Arc Hydro tools was introduced in 2012 with the goal of standardizing efficient way to analyze hydrologic data (Djokic, 2008). Recently, GIS-based hydrological models such as PCSWMM, HEC-RAS etc. has been used to perform a detailed analysis and modelling. An approach which involves detailed analysis and modelling using such hydrological models is generally beyond the local government's budget, experience and scope of work. As a compromise, through integration of spatial data like street inlets and buildings with Digital Elevation Model (DEM) using Arc Hydro tools, a correct direction of drainage path in urban area can be derived.

This study will focus on using GIS and Arc Hydro tools to determine the overland flow path in an urban catchment in Lomma municipality, Sweden.

1.1 Objectives of the study

In this study stream network and catchment will be modelled based on high resolution DEM in ArcGIS. Flow Direction assignment for the study area will be performed using two flow direction algorithms. In Deterministic eight-nodes algorithm (D8), developed by (Jenson & Domingue, 1988) flow of water from a cell in a 3 X 3 moving window is directed to only one steepest descend of each of the eight nearest neighbouring cells. The Triangular Form Based Multiple Flow algorithm (TFM) on the other hand, allows overland flow to be distributed to all lower cells surrounding a centre cell (Pilesjo & Hasan, 2014). A 10 year return rainfall event of 1-hour duration will be estimated for the modelling. A 10 year return rainfall is an event of such size that, the average time between events of equal or greater magnitude is 10 years. A 10-year event has a probability of 0.1 or 10% of being equalled or exceeded in any one year (Bedient et.al, 1948).

The primary objectives of this study are the following:

1. To investigate if the existing drainage system of the study area has satisfactory conveyance capability for runoff volume during a 10 year return rainfall events?
2. To develop simplified GIS-based models using D8 and TFM flow direction algorithms and simulate spatial extent of inundation when the capacity of the drainage systems conveyance is superseded.
3. To evaluate the extent of inundation generated by the developed simplified GIS-based models.

The key research question that this study attempts to address is.

- Are simplified GIS- models capable to produce reasonable outcome, using a high resolution DEM and additional information on urban flows as input data?

1.2 The study area

The study area Lomma town is found in Lomma municipality, Skåne county, Sweden. It is located at the coast East of Lund and North of Malmö. **Figure 1** below shows the geographical location of Skåne region and the study area in Sweden. The study area covers an area of approximately 6.31 km^2 and the terrain is almost flat. According to the size of the population as of December 31, 2005 there are 8820 inhabitants in Lomma town (Ana & Möllers, 2006). The choice of the study area is based on two main reasons:

- In the old industrial area along the river, new apartments and villas are erected, it is therefore interesting to check if the existing drainage system is sufficient for this urban expansion.
- Availability of sufficient data required for the development of the model from Lomma municipality.

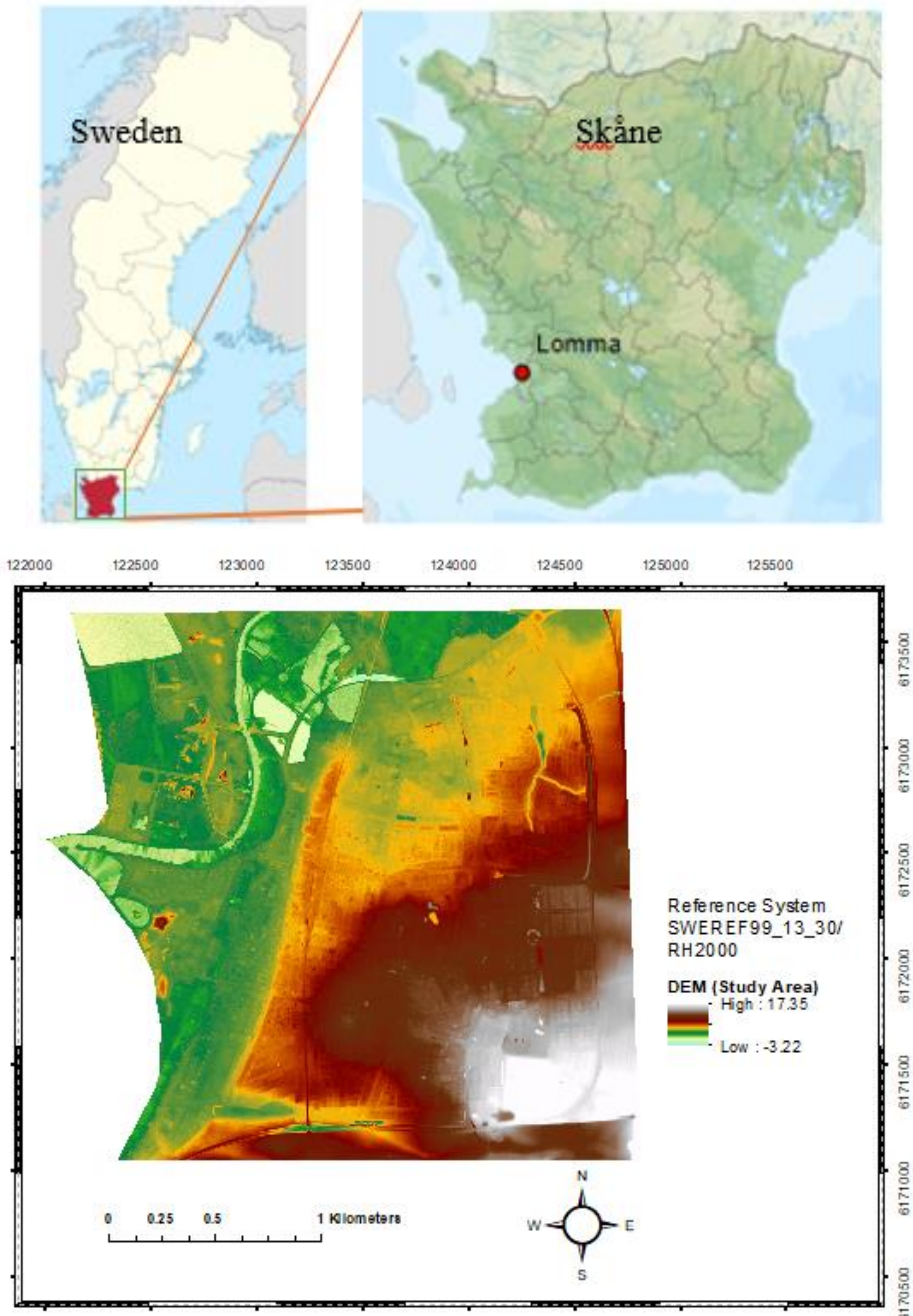

Figure 1 Skåne County with Lomma municipality (upper right) and the study area (bottom). (Source: Länsstyrelsen Skåne).

2. Theoretical background

2.1 GIS and hydrological modelling

A Geographical Information System (GIS) is defined by (Aronoff, 1989), as a computer based tool that displays, stores, analyses, retrieves, and generates spatial data. GIS software function tools such as spatial analyst tools, data management tools etc. enable the management and analysis of spatial data and attribute data. Using these GIS function tools spatially varying hydrological attributes can be calculated from high-resolution digital elevation model (DEM).

According to Sorooshian et al. (2008), models are defined as a simplified characterizations of the real world system. A model is characterised by various parameters and the model that use few parameters and least complexity to produce close results to reality is the best choice for application to the purpose in which the model is made.

The development of Rainfall-Runoff (R-R) models has helped researchers to better understand the various hydrological processes and also to simulate and predict system behaviour. Depending on the model input parameters and physical principles applied, Rainfall-Runoff model can be categorized into (1) Lumped models which consider the entire catchment as a single unit without taking into account the spatial variability and (2) Distributed models which take into account spatial variability by dividing the whole catchment into smaller units, usually square cells or triangulate irregular networks. R-R models that exclude time factor and produce output for specific time are static models, while dynamic models include time factor and produce a continuous output (Sorooshian et al., 2008).

Distributed hydrological models require spatially varying hydrological attributes as input when performing hydrological modelling. These attributes can be derived by GIS. This has led to the integration of GIS and hydrological models to develop the widely used GIS-based distributed hydrological models since the 1990s. Most GIS-based distributed hydrological models use high resolution digital elevation model (DEMs) as an input in order to accurately perform hydrological modelling. In a complex landscape such as urban environment, additional information regarding the existing drainage system is required.

2.2 Digital Elevation Model (DEM)

According to Aronoff (1989), a DEM is defined as a set of elevation measurements for locations distributed over the land surface that carries different names. A DEM is a 3-dimensional digital representation of terrain elevation data commonly used for extracting information that is essential for simulating movement of water over a terrain such as flow direction and flow accumulation. These attributes are derived based on the slope and aspect of the elevation data (Jenson & Domingue, 1988). DEMs are commonly available in raster format where elevation data is stored in an array of regularly spaced cells (O'Callaghan & Mark, 1984). Each cell contains a numeric value that represents its elevation. Continuous spatial change of elevation in natural terrains can be expressed more accurately with number of decimal places in raster DEM. This is because the structure of a DEM is defined to store floating point values. Cells in raster DEM have fixed location with a known and definable boundary (i.e. they are discrete) and their elevation value is measured from a fixed registration point which is the mean sea level therefore, they are continuous as well. This simple data structure of raster data makes it easy to manipulate the elevation variable as required (ESRI, 2011). However, the accuracy DEM is also affected by other factors such as density and distribution of the source data, the interpolation algorithm used to develop the DEM and the DEM resolution. The disadvantage of using raster DEM is that when large amount of raster data is used then the rate of processing of attribute data is slow (Li et al., 2005).

2.3 Arc Hydro Software

Arc Hydro is a data model and toolset which can be used for integrating geospatial and temporal water resource information and processing it within ESRI’s ArcGIS geographic information system (Maidment, 2004). Arc Hydro was introduced in 2002 with a goal of standardizing an efficient way to analyze hydrologic data. The two main components in Arc Hydro are Arc Hydro Data Model and Arc Hydro tools (Li, 2014). These components of Arc Hydro are used to determine and analyse watershed characteristics such as stream network, flow length, catchments and channel networks from DEMs (Li, 2014). For input into Arc Hydro, terrain must be represented as DEM in raster form, i.e. the DEM and its derivatives should be in ESRI GRID format. In case of more complex processes, for example analysing flooding in urban environment in which existing drainage structures are required superimposed into a DEM, additional vector data representing these structures is needed. All vector layers should be stored in the ESRI (geodatabase) feature class format (Djokic, 2008). In such cases, Arc Hydro enables integrating the raster DEM and vector data using the Arc Hydro tools within the terrain pre-processing menu, into a single operational data system (ESRI, 2004).

2.4 DEM pre-processing in Arc Hydro tools

Terrain pre-processing is important data preparation step in any water resource analysis. The purpose of pre-processing a DEM is (1) to develop a hydrologically correct DEM (HydroDEM) and (2) to develop a drainage pattern that represents correct flow routing in the area under investigation from the HydroDEM (Djokic, 2008). HydroDEM is developed by filling the sinks present in the raw DEM. Once HydroDEM is developed then hydrologically relevant terrain attributes such as flow direction and flow accumulated can be extracted. In HydroDEM water flowing over the surface will continues to flow downstream therefore it can be used for simulating flow of water over a terrain.

2.4.1 Fill sinks

Most DEMs contain many depressions or sinks. Depressions in DEMs are cells having elevation value lower than elevation of all neighbouring cells. Depressions can be single cell (pits) or more than one depression cells that are adjacent to each other. Most of the depressions in DEMs are spurious which arise from errors in the source data or its handling for example the interpolation techniques used to generate the DEM. But some depressions can be real terrain features such as quarries (Martz & Garbrecht, 1993). The presence of spurious sinks in DEM can complicate flow routing by disconnecting the drainage network. Therefore, accurate simulation of hydrologic flow is impossible before sinks are treated properly with sink removing algorithms. Sinks are filled in order to enforce water in the sinks to flow towards downstream direction in the DEM spatial domain (Pan et al, 2012; Jenson and Dominique, 1988).

According to Pan et al. (2012), methods for filling sinks are classified into two. The first type increase elevation of sink cell until it reaches elevation of the lowest boundary cell which has outflow direction. Fill function tool found in ArcGIS which is developed by (Jenson & Domingue, 1988), is an example of this type (Pan, et al., 2012). The second type re-compute and replace the elevation of each sink cell in the DEM in order to create a DEM with all grid cells in it having a positive downward slope. Examples of this type are the algorithms developed by (Hutchinson, 1989), and (Soille, 2004). Illustration of sink cell before and after it is treated with Fill tool in ArcGIS is shown in **Figure 2**.

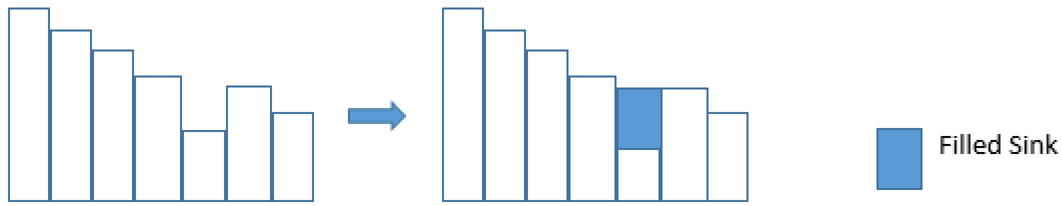

Figure 2 Illustration of sink cell before and after running Fill tool.

2.4.2 Build Walls

Due to the presence of buildings in urban area, there is big elevation difference in a relatively small area. Interpolation of elevation data that is required to produce DEM cannot be carried out successfully unless such big elevation differences are filtered out (Klok, 2012). Due to this filtering process, DEMs do not contain elevation of building. Therefore, DEM has to be modified when used for hydrological modelling in urban catchment. One way of doing this is to create walls on the DEM using Build Walls tool in Arc Hydro tools/DEM manipulation menu. The tool uses building polygons as input and creates walls at the boundary of selected polygons (ESRI, 2011). Once walls are created, the area bound by the walls has to be filled so that they will not be considered as sinks.

2.5 Flow direction algorithms

According to Zhou et.al, (2011), flow direction indicates how overland flow is distributed over a catchment and is key parameter when performing hydrological modelling. Flow direction assignment over catchment can be done from DEM, but in this case parameters such as infiltration and friction are not considered (Beven & Moore, 1993). Based on how flow is distributed from one cell to another cell in a 3 x 3 moving window, there are two types of flow direction algorithms (1) Single flow direction (SFD) algorithm, (2) Multiple flow algorithm (MFD).

In single flow direction algorithm, flow of water is restricted to only one down-hill direction at a time, even though in reality the flow may be proportionally distributed into two or more adjacent down-stream cells. Multiple flow algorithm on the other hand flow of water on a grid DEM can be distributed into more than one flow direction (Zhou, et al., 2011). Single flow direction algorithm D8 (deterministic 8 node algorithm) and multiple flow direction algorithm TFM (Triangular Form based Multiple Flow algorithm) are discussed in the following sections. **Figure 3** below illustrates how single flow direction and multiple flow direction algorithms disperse flow of water over a terrain represented as DEM.

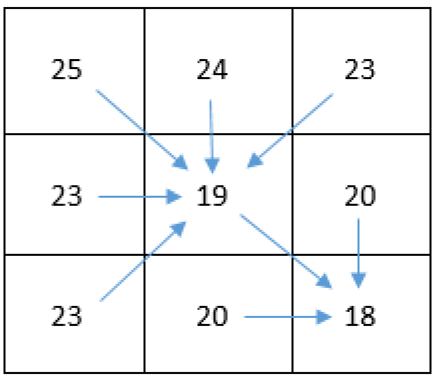

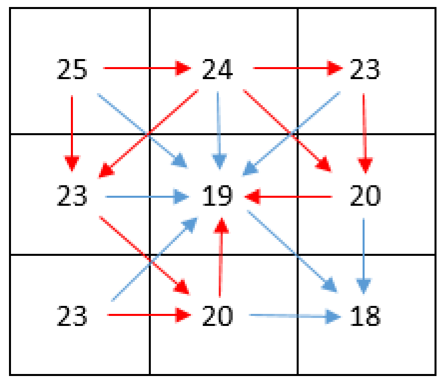

Figure 3 single flow direction algorithm SFD (left) where flow of water from a cell is directed to only one steepest downstream cell. Multiple flow direction algorithm MFD (right) in which direction of flow from a cell can be directed to more than one downstream cells.

2.5.1 Deterministic eight-node (D8) algorithm

D8 (deterministic eight-node) algorithm was introduced by (O'Callaghan & Mark, 1984) and then improved by (Jenson & Domingue, 1988). It has been most widely used algorithm for drainage network extraction and catchment delineation. D8 algorithm directs flow from a cell to the direction of steepest descent of each of the eight nearest neighbouring cells. In D8 algorithm, slope between a focus cell and one of its neighbours is calculated by dividing elevation difference to the distance between them expressed in percentage. To calculate distance, the algorithm treats the cells as points located at the centre of each cell. Therefore, the four diagonal neighbours are 1.414214 times as far from the other 4-connected orthogonal neighbours (Jenson and Domingue, 1988; O'Callaghan and Mark, 1984). Flow direction in D8 method is calculated using Formula (1) below:

$$\text{Drop} = (\Delta Z / d) * 100 \tag{1}$$

Where ΔZ = elevation difference

d = distance

Flow direction for cells at the edges of a raster is assigned automatically based on the slope with maximum gradient. Once the direction of steepest descent grid is calculated, ArcGIS assigns codes as shown in **Figure 4** below.

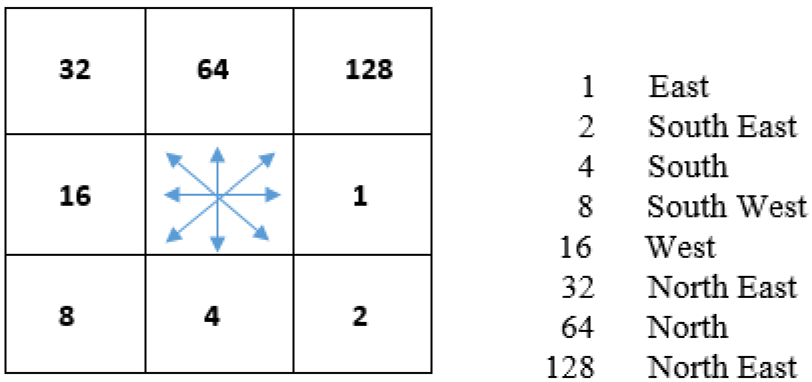

Figure 4 Coding the direction of flow to the eight adjacent cells in Deterministic eight-node (D8) algorithm.

The advantages of D8 algorithm are its simplicity, consistent flow patterns, and spatial representation of sub catchments (Tarboton & Ames, 2001). However, it may not be realistic to assume that water will flow only towards one of the eight directions, because in reality flow may be proportionally distributed to two or more adjacent down-stream cells (Pourali, et al., 2014).

2.5.2 Triangular Form Based Multiple Flow Algorithm (TFM)

TFM algorithm was developed by (Pilesjo & Hasan, 2014) and it is one of the several algorithms developed in order to overcome the limitation of SFD methods. TFM is based on multiple flow distribution allowing overland flow to all lower cells surrounding a centre cell. TFM algorithm models movement of water over a grid cell before flow direction assignment between one cell and its neighbours is estimated. This is done by dividing each grid cell into eight local triangular facets

(Pilesjo & Hasan, 2014). According to Pilesjö and Hasan (2014), the 8 planar triangular facets are created using midpoints of the centre cell and midpoints of two adjacent cells. The centre cell is finally represented by 8 triangular facets whose area is 1/8 of the cell size as shown in Figure 5 below.

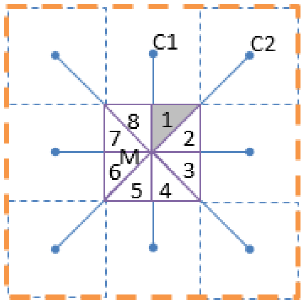

Figure 5 Illustration of subdivision of a centre cell into 8 triangular facets in Triangular Form based Multiple flow Direction (TFM) algorithm, denoted 1 – 8. Source: (Pilesjo & Hasan, 2014). The figure is reprinted with permission from (Piljesjö & Hasan 2014).

There are four possible ways of water movement from a facet denoted as follows:

1. **Stay**, if all water from a facet is directed to a neighbouring cell and happens (aspect = 0-45).
2. **Move**, if water from a facet is directed to only one facet (aspect = 90-180 or 225-270).
3. **Internal** split, if the flow between two facets is towards each other (aspect =180-225).
4. **Split**, if part of flow from a facet is to another facet and part to adjacent cell (aspect = 45-90).

These possible ways of water movement is illustrated in **Figure 6** below.

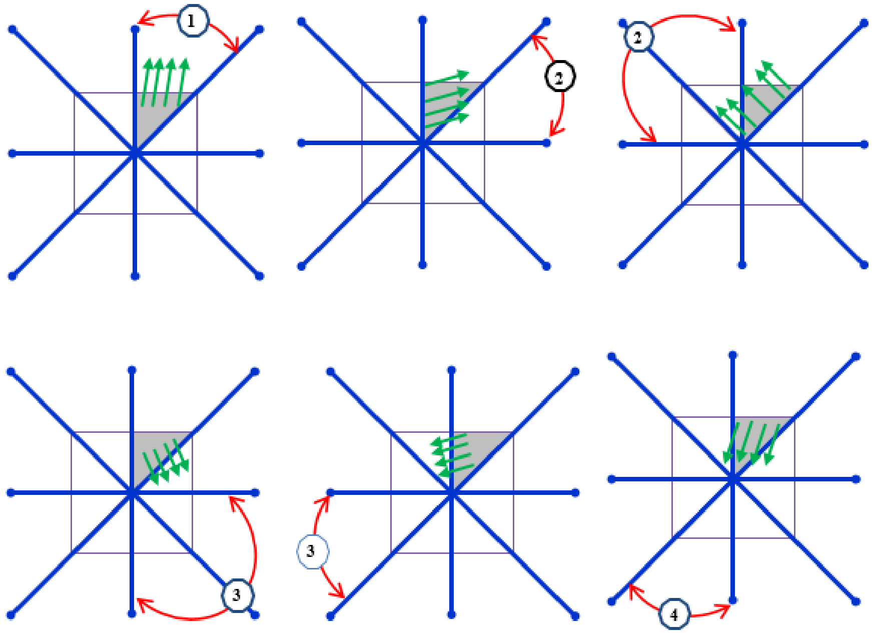

Figure 6 Different ways of water flowing from a facet at different aspects. 1, 2, 3, and 4 represent stay, move, internal split and split respectively. Source: (Pilesjo & Hasan, 2014). The figure is reprinted with permission from (Piljesjö & Hasan 2014).

2.6 Watershed modelling in urban areas

Automatic delineation of sub-catchments and their respective pour points cannot be used for modelling watersheds in urban areas. This is because in urban areas the location of street inlets has to be known accurately and used as pour points for delineating the sub-catchment boundaries (Kunapo, et al., 2007). For this reason, the DEM derived from LIDAR data could not offer an immediate use for sub-catchment delineation. Therefore, appropriate spatial data integration is required in the terrain processing to embed storm water drainage flow in urban catchment. Sub-catchments derived using street inlet points and DEM will represent both the topography and the existing drainage network (Kunapo, et al., 2007). Watershed tool in ArcGIS spatial analyst meets this objective. Batch watershed delineation found in Arc Hydro tools can also be used, in both cases street inlet points must be specified as pour points in order to delineate their respective sub catchments.

3. Data and Software Used

3.1 Digital Elevation Model (DEM)

A 2m resolution DEM data was provided by Lomma municipality covering a larger area as shown in **Figure 7**. Information regarding how the DEM was produced is documented in the Metadata PDF file that is attached with the LIDAR data describing the data acquisition, preparation and calibration procedures. Laser Scanning was performed by Blom Geomatics AS on 2008-04-29 and 2008-05-06. Lantmäteriet Metria performed signalling and measurement of the control surfaces and terrain profiles. Other processing took place at Blom Sweden's office in Sollentuna. Sensor specifications and data capture parameters are as shown in the **Table 1** below.

Table 1 Sensor specifications and data capture parameters during the development of the DEM.

Item	Specification
System (Sensor)	Optech ALTM Gemini
Altitude	1100 m
Laser Pulse Frequency	100,000 Hz
Scanning frequency	43 Hz
String Width	900 m
Point Density	1.5 pt./m^2
Aircraft's GPS positioning	+ INS

Average dz is +0004 m.

Statistics by height alignment: square error of 0.098m and standard deviation 0.098m.

The DEM was delivered to Lomma Municipality in reference SWEREF99_13_30 / RH2000 in DEM grid ArcMap raster. SWEREF99_13_30 was used throughout this study because all vector data **Section 3.3** received from Lomma Municipality has the same coordinate system. The DEM was clipped into the area of interest in ArcMap as shown in **Figure 8** below.

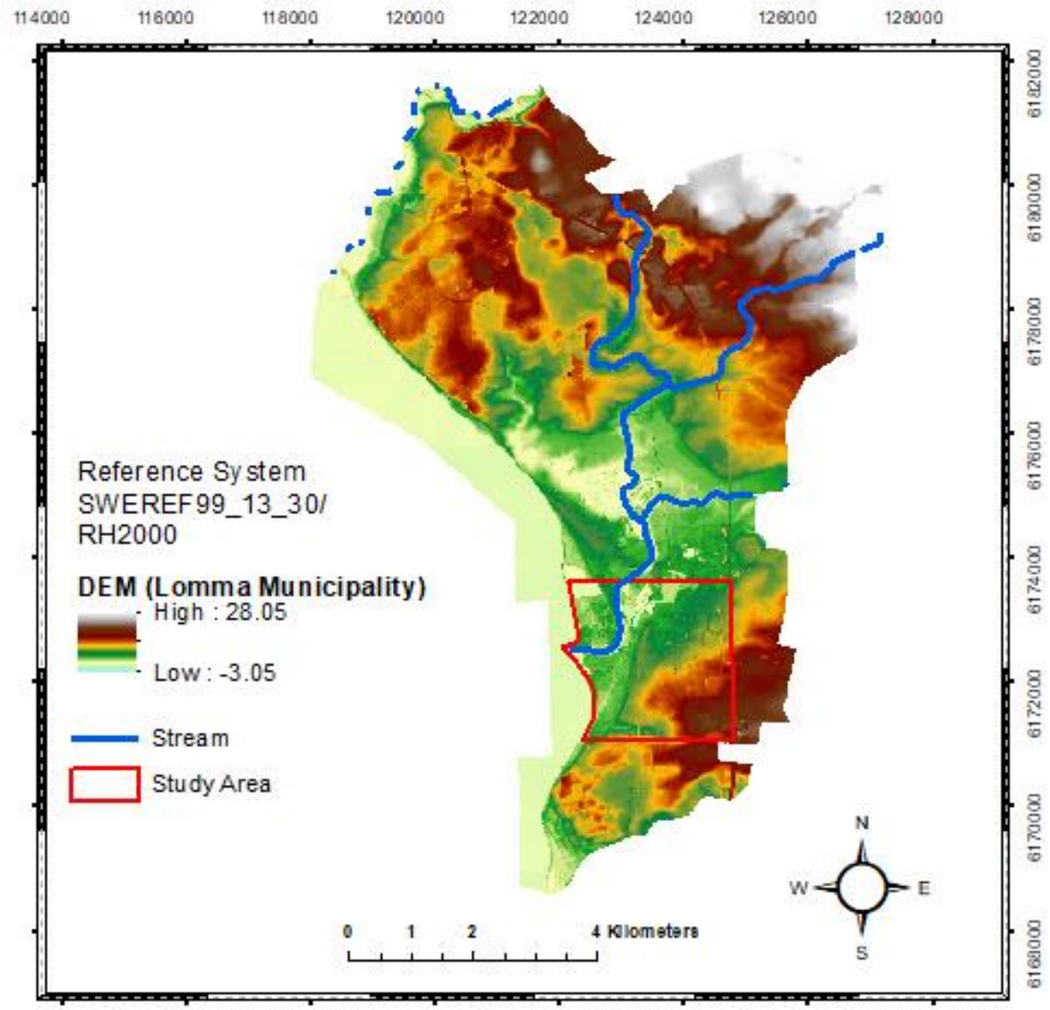

Figure 7 Raw DEM data covering Lomma municipality with the study area marked in (Red line) and streams marked in (blue line).

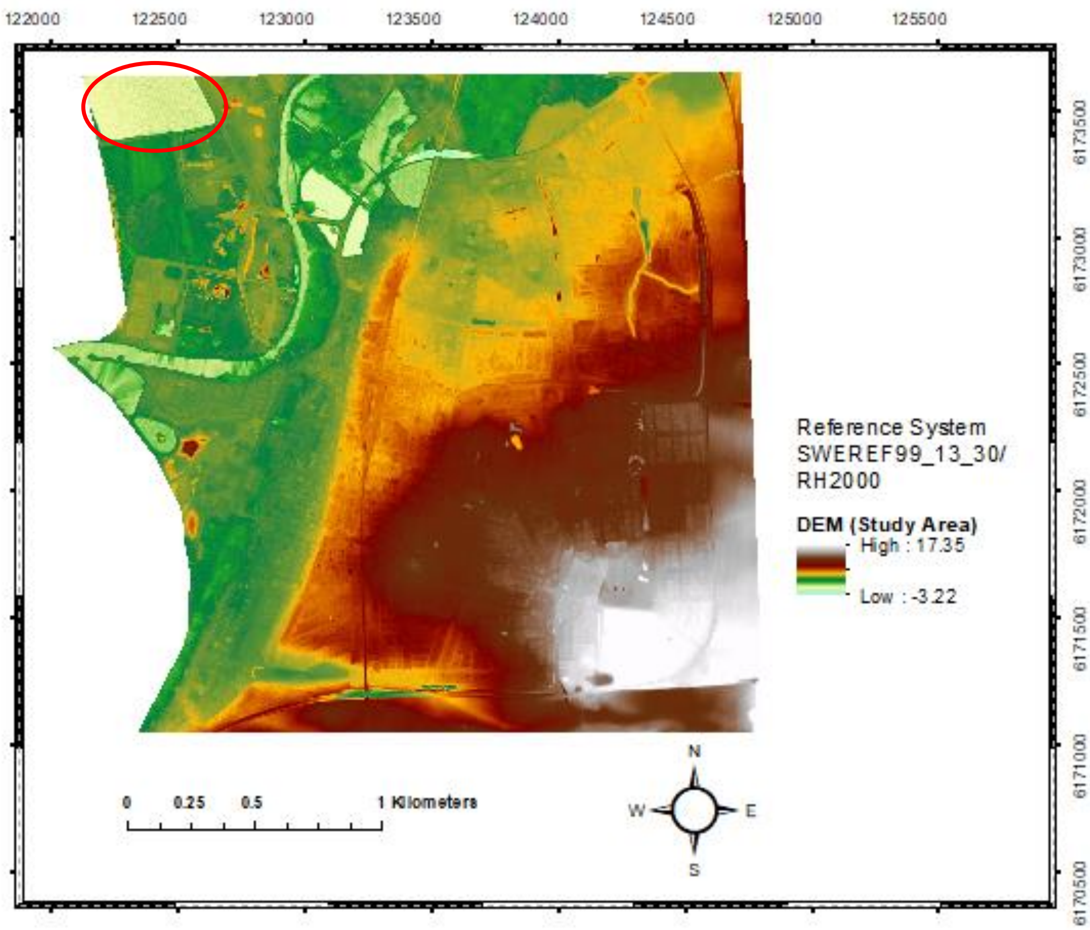

Figure 8 DEM of the study area covering 6.31 km^2. The DEM is made up of 2m X 2m resolution cells. The area with lowest elevation value (-3.22m) marked in red circle was used as a brickyard by AB Lomma Brick Factory in mid-1970s.

3.2 Ortho photo

A multispectral Ortho image of 1-meter resolution was received from Lantmäteriet in SWEREF99_TM coordinate system and was projected into SWEREF99_13_30 in ArcMap as shown in **Figure 9.**

Figure 9 Ortho photo of the study area.

3.3 AutoCAD data

AutoCAD data describing the existing drainage system of the study area including buildings, cadastre, lakes and location of street inlets was provided by Lomma municipality in SWREF99_13_30 coordinate system. 2338 street inlet points were used in the analysis.

The AutoCAD data was converted into ArcGIS shape file in FME software. The data was clipped and imported to ArcMap and is presented in **Figure 10**.

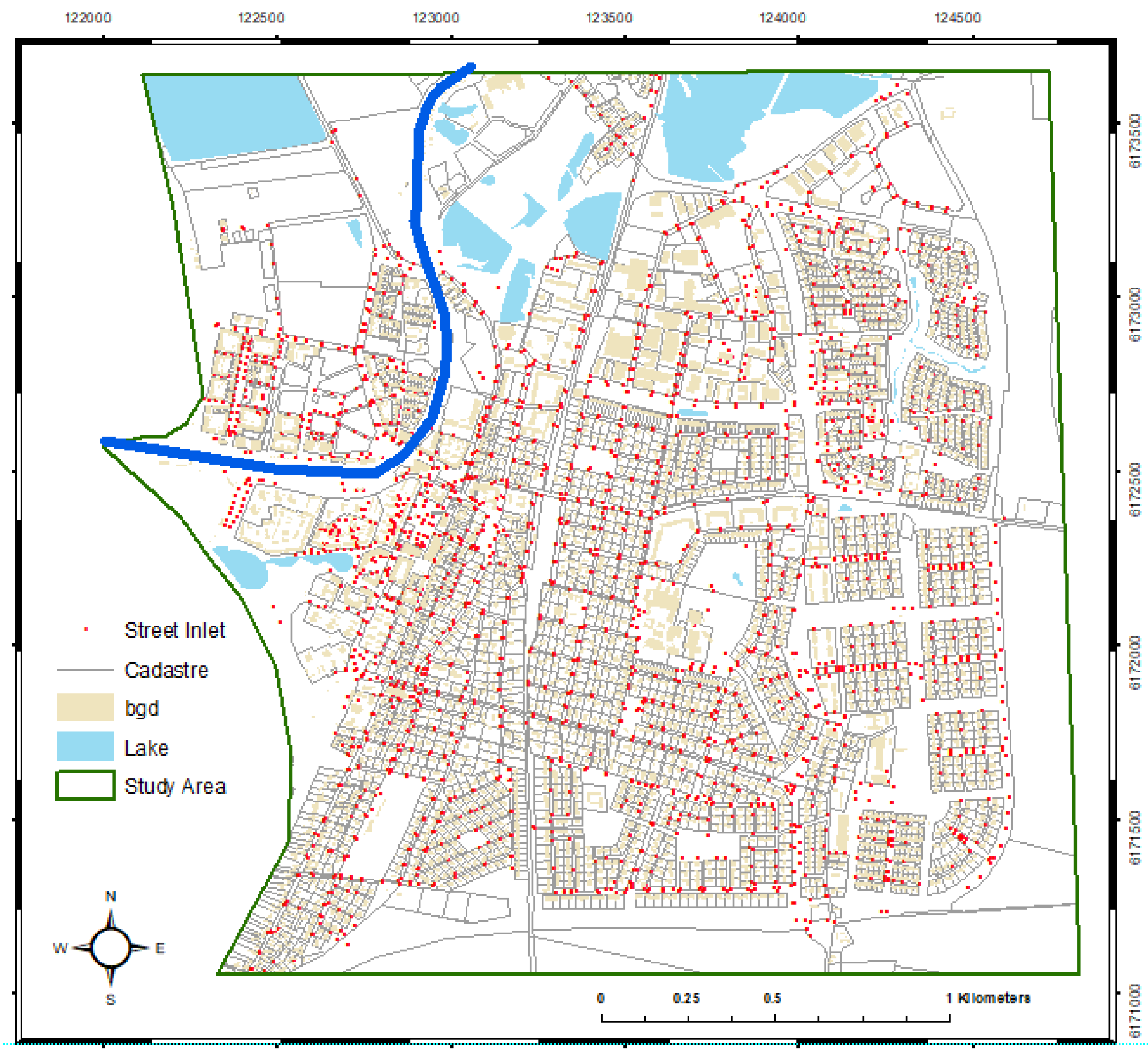

Figure 10 AutoCAD data received from Lomma municipality including street inlets (Red points), cadastre (Green lines), steam (Dark Blue), and lakes (Sky Blue) provided by Lomma municipality in SWEREF99_13_00 coordinate system.

3.4 Precipitation data

The existing drainage system of the study area is built by Swedish standard to cope with rainfall of 10-year return period of 30 min duration. According to Bedient et.al, (1948), a return period is defined as an annual maximum event that has a return period (or recurrence interval) of T-year, if this value is equalled or exceeded once, on the average, every T-year. 10-year return rainfall for the study area is estimated according to the following. Firstly, 1-hour rainfall data record for period of 1995-2016 was downloaded from Swedish Meteorological and Hydrological Institute website available at http://opendata-download-metobs.smhi.se/explore/ as shown in **Figure 11.** Since there is no meteorological station inside the study area, the closest meteorological station to the study area with 1-hour rainfall data i.e. (Malmö A), located at latitude 55.5714, longitude 13.0734 (SWEREF_99 geodetic reference system) was chosen for data collection. Using this rainfall data, 10-year return period rainfall was calculated using Hazen method (Urías, et al., 2007) in Excel spread sheet.

Hazen method was chosen for probability analysis in this study based on the recommendation of (Bhavsar & Patel, 2015). Their research compares 5 empirical methods namely California method, Weibull method, Hazen method, Cbegodayev method and Blom method. All the empirical methods are similar in the technique they use for sorting rainfall data i.e. the given annual peak rainfall is arranged in descending order and rank is assigned to each rainfall, 1 being assigned for the highest rainfall. However, they differ in the formula that they use to calculate probability of occurrence. The formula used in Hazen method is as shown in Equation 2. For detailed description about the other empirical formulas refer a published research article by Bhavsar and Patel (2015), titled ‘’Peak Flood Probability Analysis for Sabarmati River, Gandhinagar.’’. Result of their research shows that Hazen method gives the most probable peak discharge value and is therefore recommended for practical use in probability analysis.

The calculated 10-year return rainfall in this study is **25.9** mm/hr as shown below. To check if this calculated value is reliable, it was compared with 10-year return rainfall of Lund and Burlovs. The 10-year return rainfall of these location was calculated by Svenskt Vatten (Swedish Water Service Company). Accordingly, Lund and Burlovs have 10-year return rainfall of **25.704** mm/hr and

26.964 mm/hr respectively (VA Syd, 2012). Thus, the calculated 10-year return rainfall value for Lomma using Hazen method is considered reliable. In this study 10-year return period rainfall is used for analysis because the drainage system of the study area is built by Swedish standard to cope with rains of return period of 10 years (MSB, 2014).

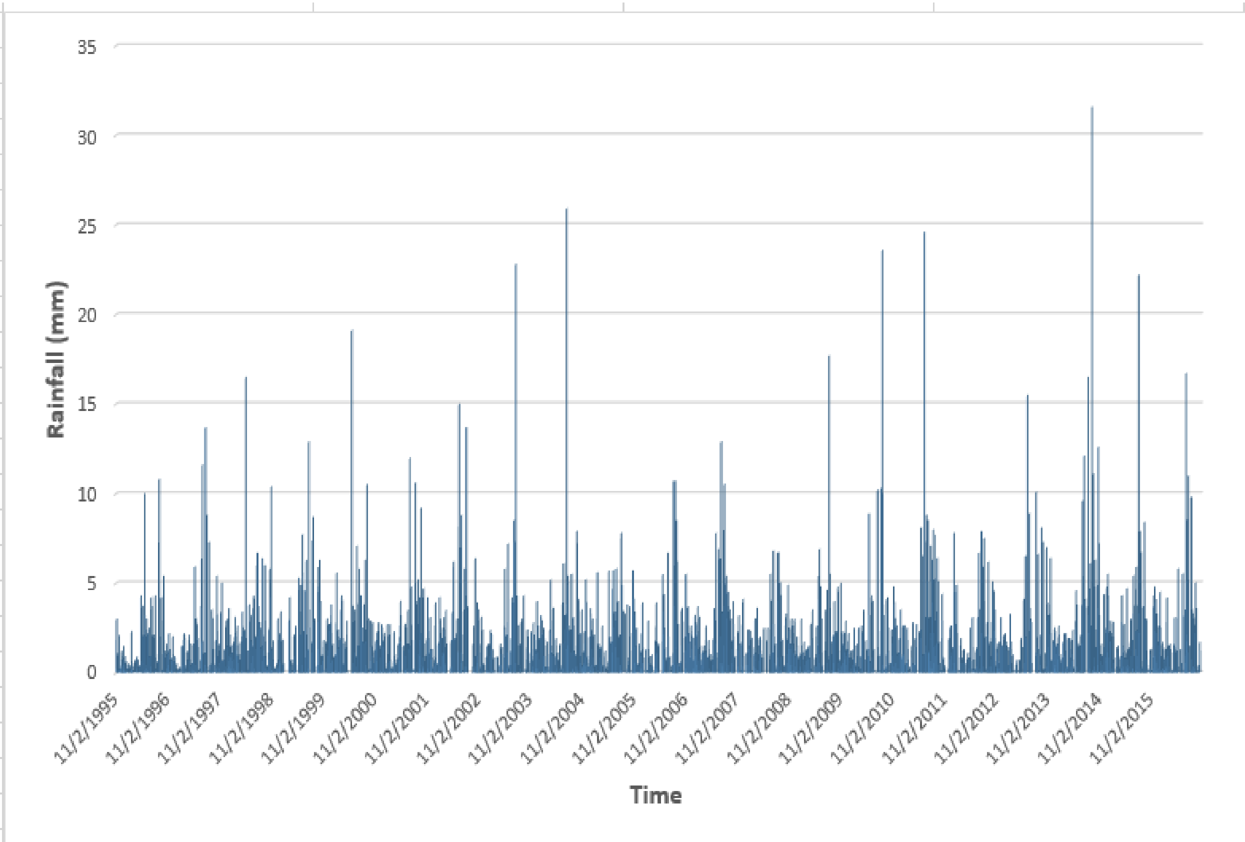

Figure 11 Showing 1-hour rainfall data for period of 1995 – 2016 downloaded from Swedish Meteorological and Hydrological Institute website (SMHI). Source: (Swedish Meteorological and Hydrological Institute).

Hazen method for calculating 10-years return rainfall

- Maximum rainfall of each year were identified by sorting the data in descending order.
- Rank the sorted rainfall data, 1 being for the highest rainfall.
- Calculate probability of occurrence (Fa) using Formula (2)

$$Fa = 100(2n-1) / 2y \quad (2)$$

Where n = the rank of each event

y = total number of events

- Calculate return period using Formula (3)

$$\text{Return period} = RP = 100/Fa \tag{3}$$

Rainfall data sorting and development of 10-year return rainfall event using Hazen method is shown in **Table 2** below.

Table 2 Showing rainfall data sorting and development of 10-year return rainfall; the estimated 10-year return rainfall of 1-hour duration is **25.9 mm** (Red circle).

Year	Rainfall(mm)	rank	Fa	Return Period
2014	31.6	1	4.55	22
2004	25.9	2	9.09	11
2011	24.6	3	13.64	7
2010	23.6	4	18.18	6
2003	22.8	5	22.73	4
2015	22.2	6	27.27	4
2000	19.1	7	31.82	3
2009	17.7	8	36.36	3
2016	16.7	9	40.91	2
1998	16.5	10	45.45	2
2013	15.5	11	50.00	2
2002	15	12	54.55	2
1997	13.7	13	59.09	2
1999	12.9	14	63.64	2
2007	12.9	15	68.18	1
2001	12	16	72.73	1
1996	10.8	17	77.27	1
2006	10.7	18	81.82	1
2012	7.9	19	86.36	1
2005	7.8	20	90.91	1
2008	6.8	21	95.45	1
1995	3	22	100.00	1

3.5 Software

Software programmes that were used to store and analyse the collected data are the following ArcGIS 10.3, Arc Hydro, Matlab, FME, and Excel.

4. Methodology

4.1 Model assumptions

According to Djokic & Maidment (1991), there are three ways in which water in urban catchment flows (1) diffused overland flow (sheet flow to the nearest drainage inlet and gap flow in the location of each inlets) (2) Concentrated overland flow and (3) Concentrated flow in a man-made network system such as storm water collection. If analysis takes into account the three types of water movement, then it is referred as a gap flow (Argue, 1986). This type of detailed analysis is often performed by a consultant. In addition, it is outside of the scope of this study. Alternatively, it is possible to assume the following in order to include flow consumed by street inlets in urban environment:

1. Street inlets intercept some of the flow from their respective catchments and the remaining flows over the surface until it reaches another inlet downstream. According to Brown et.al, (2009), street inlets are described as locations where water that was flowing over land is concentrated and transferred to the storm water drainage network. **Figure 12** shows four types of street inlets. Due to lack of information regarding the flow interception capacity of the street inlets in Lomma, it has to be estimated according to the following. Firstly, the size of street inlets in the study area was measured and majority of them were found to be **42 cm X 40 cm** grate type inlets as shown in **Figure 13**. Then, the average longitudinal slope of streets in the study area was estimated in ArcMap. To do this, elevation and distance of two points along the streets in the DEM was taken then the longitudinal slope was calculated using Formula (4).

$$\text{Slope} = (\text{rise} / \text{distance}) * 100 \qquad (4)$$

   Estimated average longitudinal slope is **0.04 m**. This result is average longitudinal street slope of 15 calculations randomly taken in different parts inside the study area. Finally, this parameter was used to estimate interception capacity of inlets based on research publication by (Brown, et al., 2009). According to the published research, a 60 cm x 60 cm grate type street inlet constructed along streets with longitudinal slope between 4-6 percent can consume **0.06 m³/sec Figure 14**. In terms of area, a street inlet in Lomma is 50% less than that of 60 cm X 60 cm inlet from the chart thus, 50% of 0.063 m^3 which is **0.035 m^3** is assumed to be the flow interception capacity of street inlets in the study area.

2. Precipitation over the entire study area is assumed to be same so that each grid cell receives the same amount of water.
3. Infiltration capacity and other forms of losses are assumed to be zero for the study area.

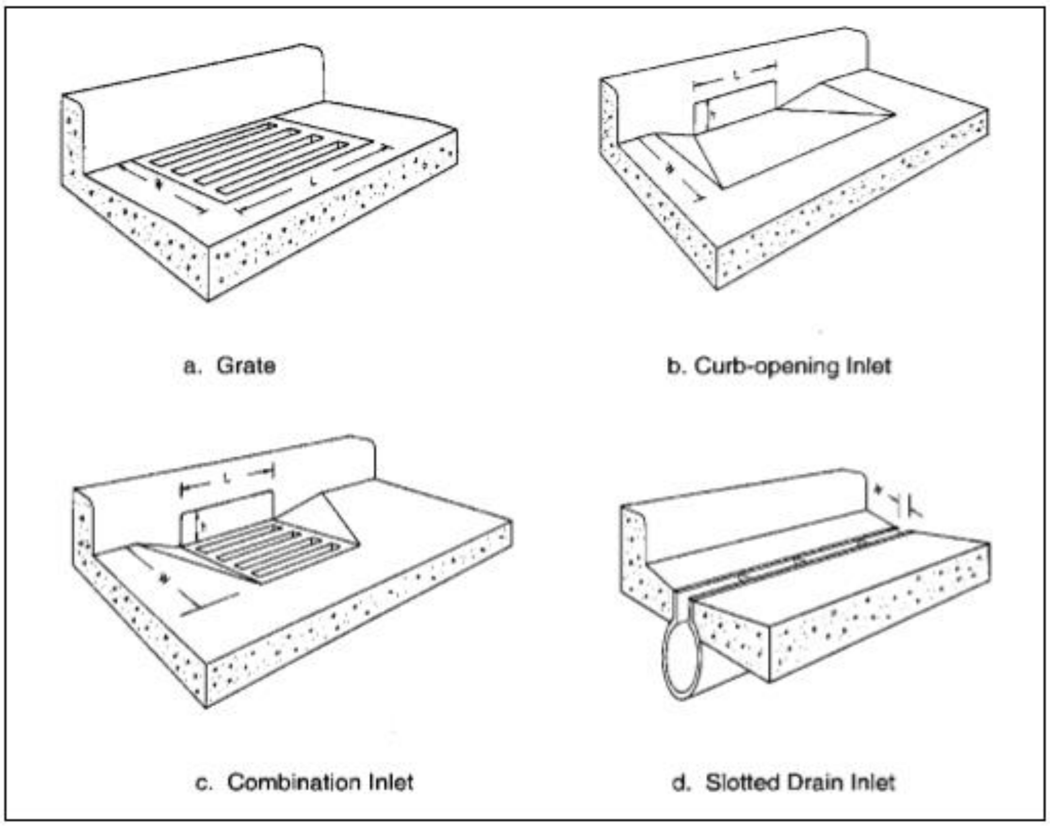

Figure 12 Four different types of inlets. Source: (Brown et al., 2009). The majority of street inlets in Lomma are 42 cm X 40 cm Grate type inlets.

Figure 13 Dimensions of grate type inlets in Lomma town (42 cm X 40 cm).

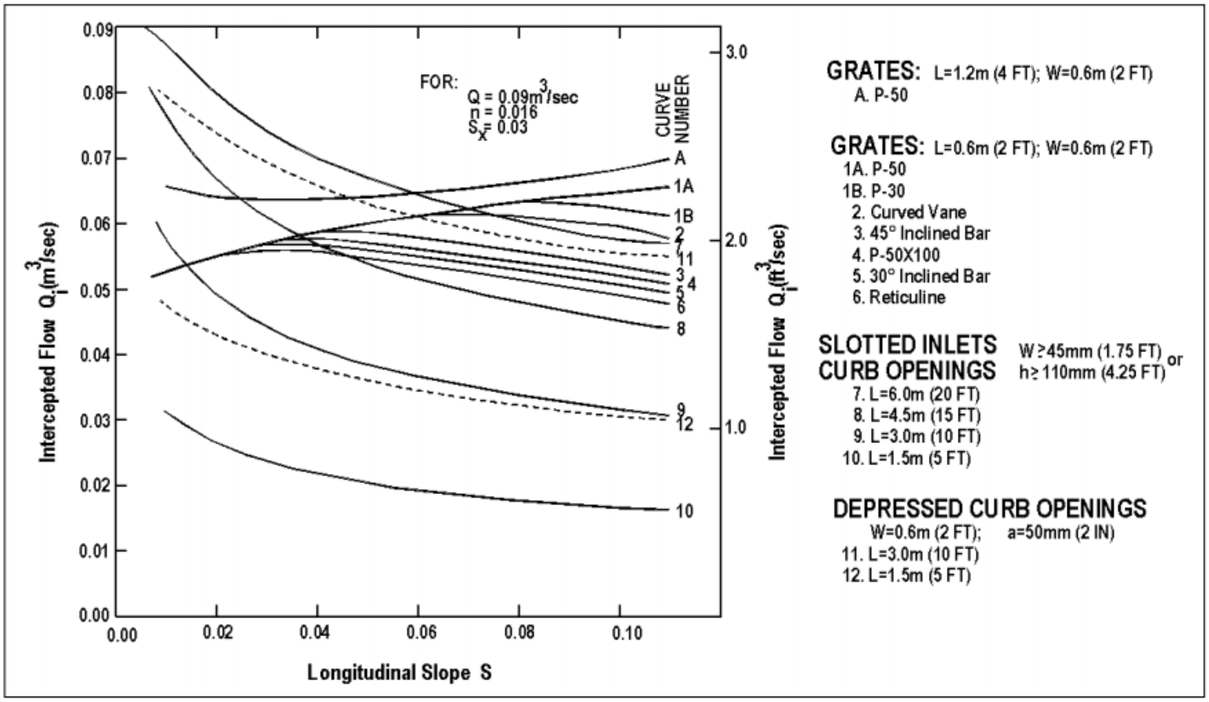

Figure 14 Comparison of inlet interception capacity vs slope of street. Source: (Brown, et al., 2009). The figure is reprinted with permission from (Brown, et al., 2009).

According to Brown et al. (2009), in order compare the interception capacity of the four different type of inlets shown in the above **Figure 12** two variables were fixed. The gutter flow was fixed to 0.09 m^3/s and cross slope of roads fixed to 3 %. But the longitudinal slope varied to 10 % as shown in **Figure14** above. The conclusions drawn from the figure above was not directly transferred for use in this study. Instead, the parameters used in the study such as longitudinal slope and dimension of street inlets were first measured for Lomma then the chart was used to estimate capacity of street inlets interception capacity based on the measured information.

4.2 Implementation of the models

One of the objectives of this study is to evaluate extent of inundation generated by using two different flow direction algorithms to calculate flow accumulation from the catchment namely, the Deterministic eight-nodes (D8) algorithm and the Triangular Form Based Multiple Flow algorithm (TFM).

D8 algorithm allows the delineation of sub-watersheds areas by defining street inlet points as input pour points. Once sub-watershed areas are delineated then flow accumulation that can be generated from each sub-watershed can be calculated. In TFM algorithm this task is not possible because the flow direction output is a matrix of 8 files and cannot be used as input for sub-watershed delineation. Thus, two different approaches were applied for each algorithm according to the following.

In D8 method flow accumulation was calculated for each sub-watershed then street inlet's flow interception effect was included in the analysis. To do this, first the capacity of the street inlets to intercept flow per unit time was estimated. Then, this information was used to prepare a weight raster for later use as input weight to run flow accumulation with weight. In TFM algorithm on the other hand this was done differently. First, sinks were created on the DEM at locations of street inlets and the DEM with sinks was then used as input to run TFM algorithm in MATLAB software. The flow accumulation values at the sink cells were extracted and used to prepare a weight raster for later use as input weight to run flow accumulation with a different flow accumulation tool that can operate with negative weights. Input data such as DEM, street inlet points, building polygons utilized to develop the two models remain the same. The general steps that were taken in each approach is as shown in **Figure 15** below with orange and grey colours representing D8 and TFM method respectively.

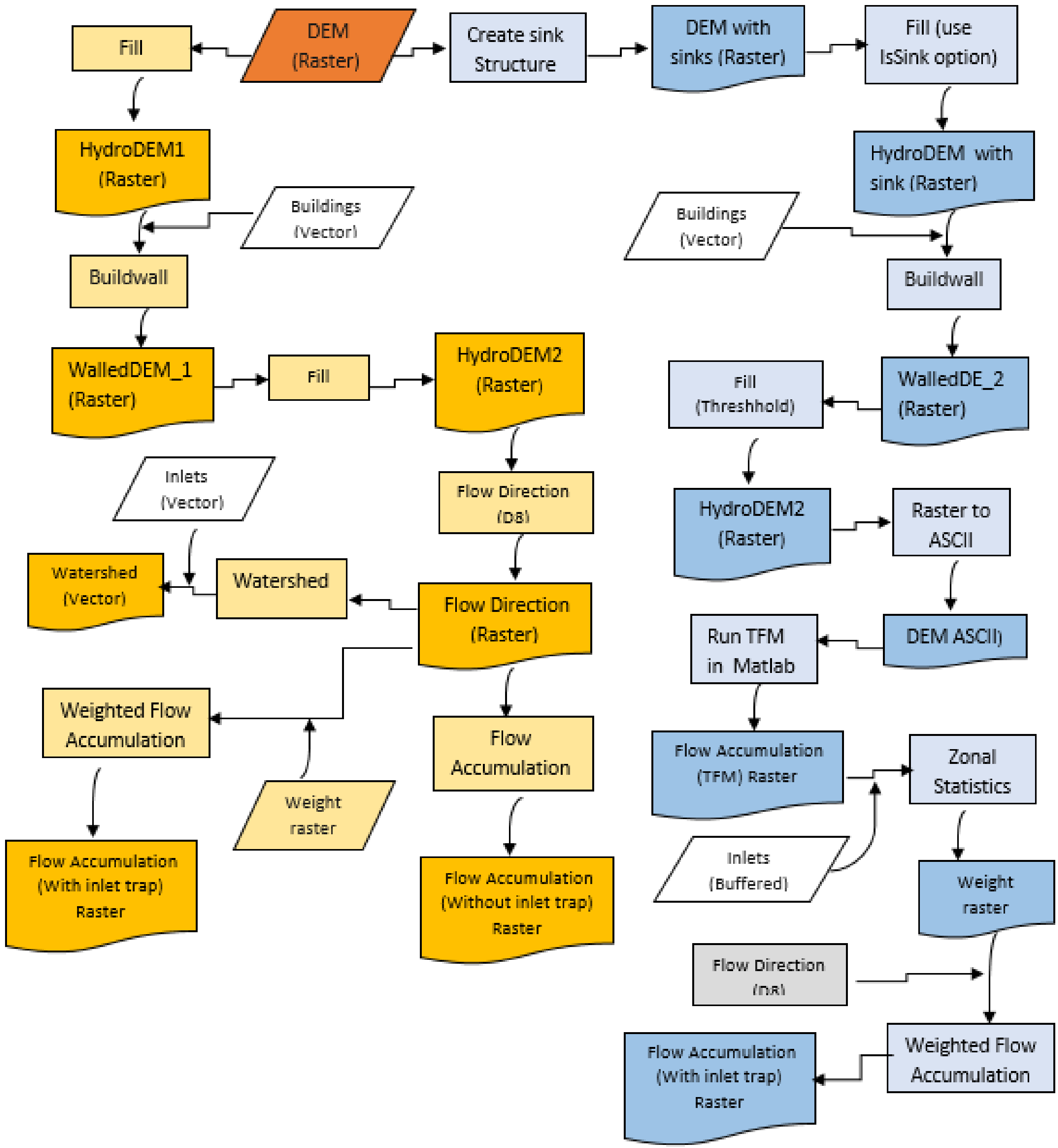

Figure 15 Showing the general work flow for Deterministic eight-nodes (D8) algorithm method (Orange) and Triangular Form based Multiple Flow Direction (TFM) algorithm method (Blue). The input raw DEM is processed with ArcGIS functionality tools to develop primary hydrological attributes such as HydroDEM, Flow Direction and Flow Accumulation without inlets trapping effect. Finally, a weight raster is generated in order to account the effect of inlets flow trapping effect by using it as input to run flow accumulation with weight.

DEM pre-processing is the first step taken to create a hydrological correct DEM (HydroDEM) in both methods. Once HydroDEM is generated, the process then continues with assignment of flow direction and flow accumulation calculation. Finally, a weight raster was prepared to include the effect of street inlets flow interception effect into the analysis. This was done by running flow accumulation with weight using the output weight raster and flow direction as inputs. However, the way the above attributes were derived in both methods is different which will be described in more detail in the following sections.

4.2.1 Generating hydrologically correct DEM

DEM pre-processing is done to create hydrologically correct DEM (HydroDEM) from which primary DEM derivatives such as flow direction and flow accumulation can be generated. DEM manipulation tools found in (Arc Hydro tools/Terrain pre-processing) such as Fill Sink, Build Walls, and Fill walled DEM were used for creating HydroDEM in both methods.

DEM pre-processing process in D8 method begins with filling the spurious sinks present in the original LIDAR DEM and output raster HydroDEM is generated in this step. However, the study area is urban and the generated HydroDEM does not have elevation of buildings. Thus, this output HydroDEM cannot be used to calculate flow direction. Therefore, elevation of buildings present in the study area was raised by creating walls at the boundary of building polygons using (Arc Hydro tools). Building polygons representing the building inside the study area were used as input to create walls. The area bound by the walls was then filled so that they will not be considered as sink (Arc Hydro tools). Output raster HydroDEM with elevation of building raised is presented in **Figure 16**. Flow direction assignment, flow accumulation calculation and sub-watershed delineation in D8 method is based on this HydroDEM.

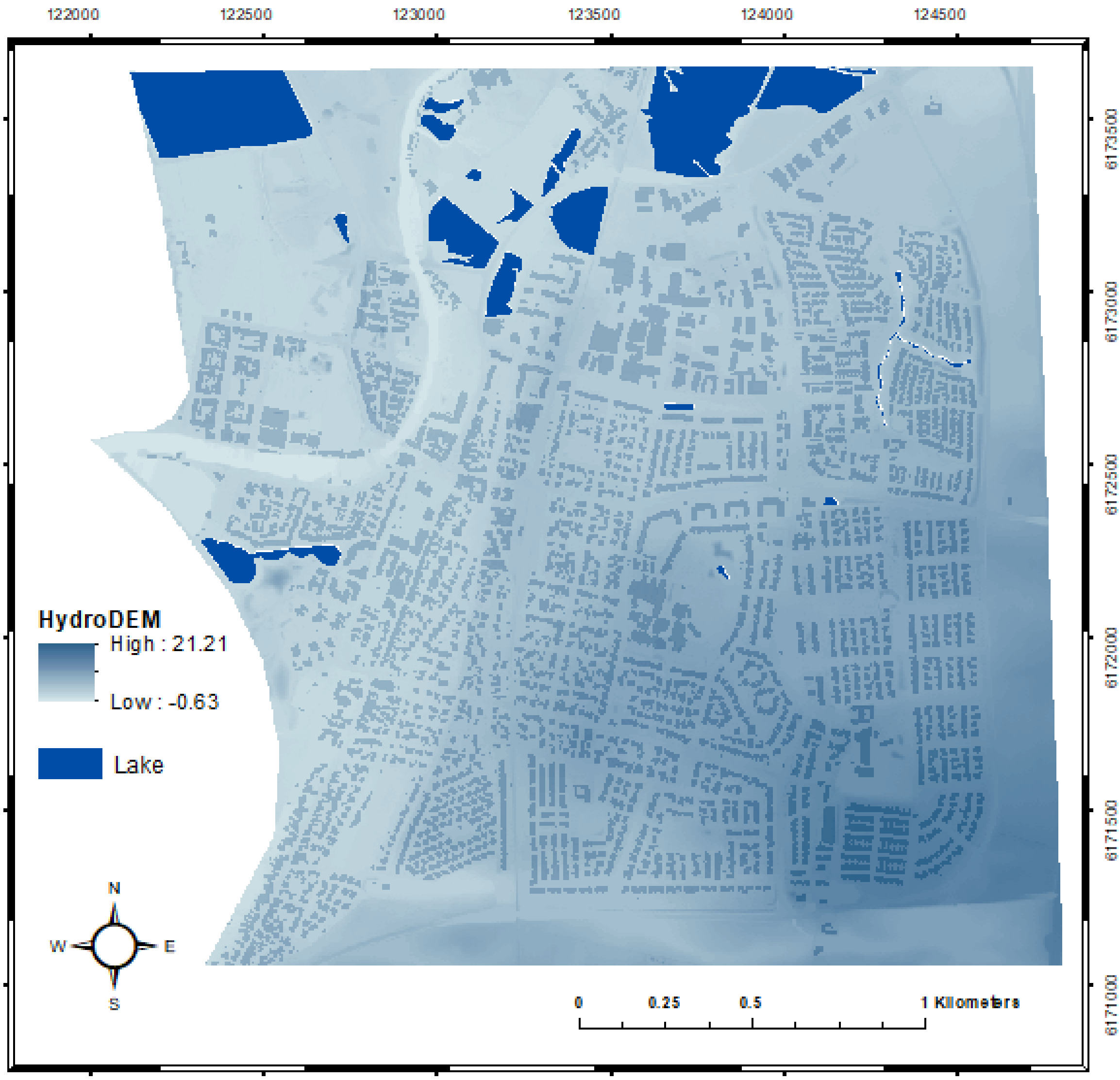

Figure 16 HydroDEM prepared by creating walls around the building polygons and filling the area bound by the walls in Arc Hydro Tools. This HydroDEM was used as input to calculated flow direction using the Deterministic eight-nodes flow algorithm (D8) in Arc Hydro tools.

In TFM method, flow direction assignment and flow accumulation calculation is performed in Matlab software. Sub-watershed delineation with defined pour points (in this case street inlets) is not possible in TFM. Therefore, a different approach was applied to develop HydrDEM as follows. Firstly, a 2 m X 2 m sink structures were created on the DEM at exactly the same location of the street inlets in the study area as follows.

- Add field in the attribute table of street inlets layer (field named elevation).
- Elevation value for sinks cells was assigned to be (-50 m)
- Convert the point layer to raster layer and use the elevation field to assign values to the output raster. Choose resolution and coordinate system to be the same as the original DEM.
- Convert the DEM raster to point.
- Extract values from output in step 1 to DEM points.
- Convert the output to raster again.
- Merge raster from step 1 and 2 and choose the mosaic operator option to be sum.

The output raster DEM with sinks cell of the study area is presented in **Figure 17** below. In order to visualise the sink cells better a more detailed figure is composed by zooming in on some part of the study area as shown in **Figure 18**.

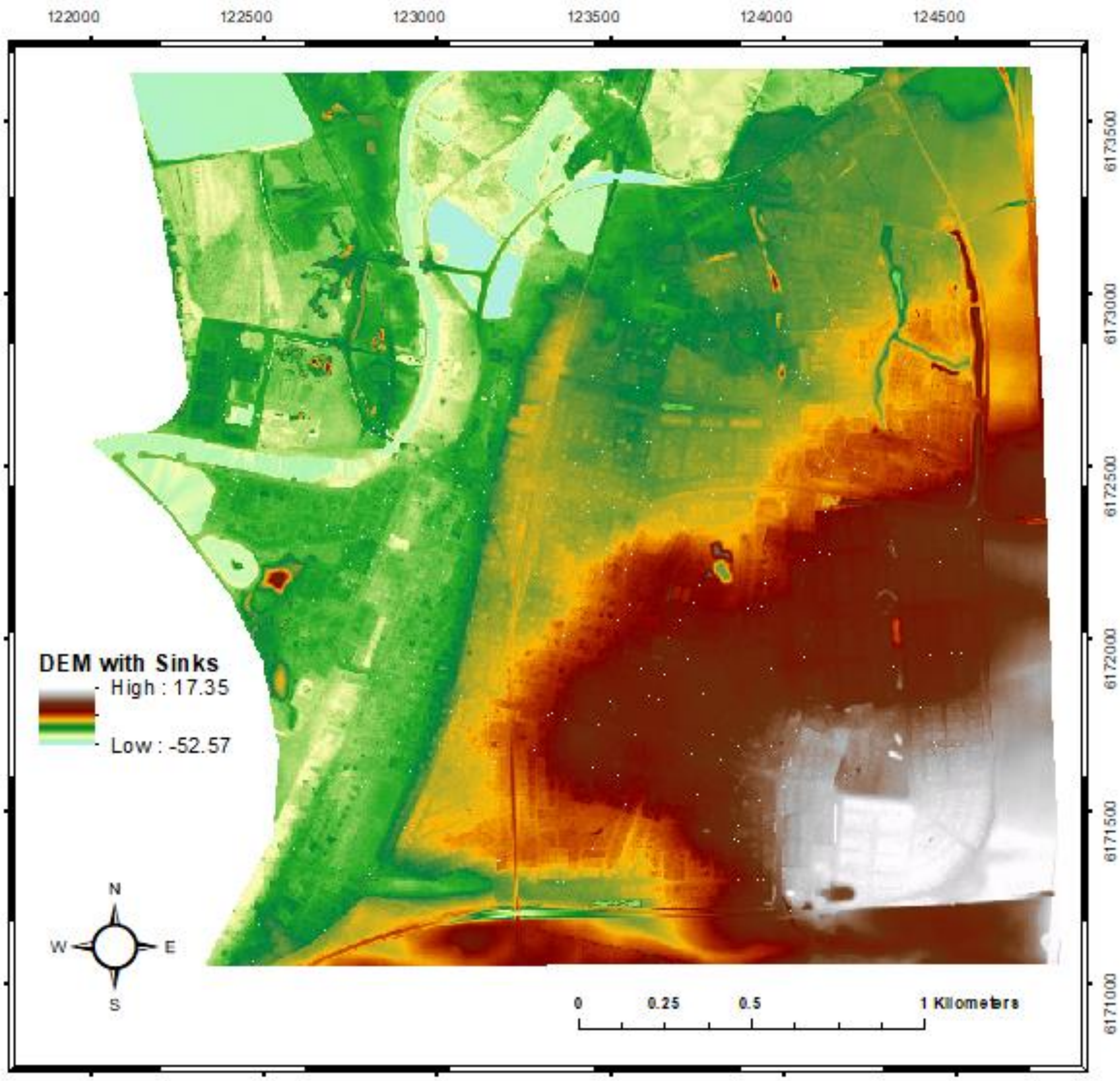

Figure 17 DEM with sink structures created on it (Grey dots) at exactly the same locations of street inlet points.

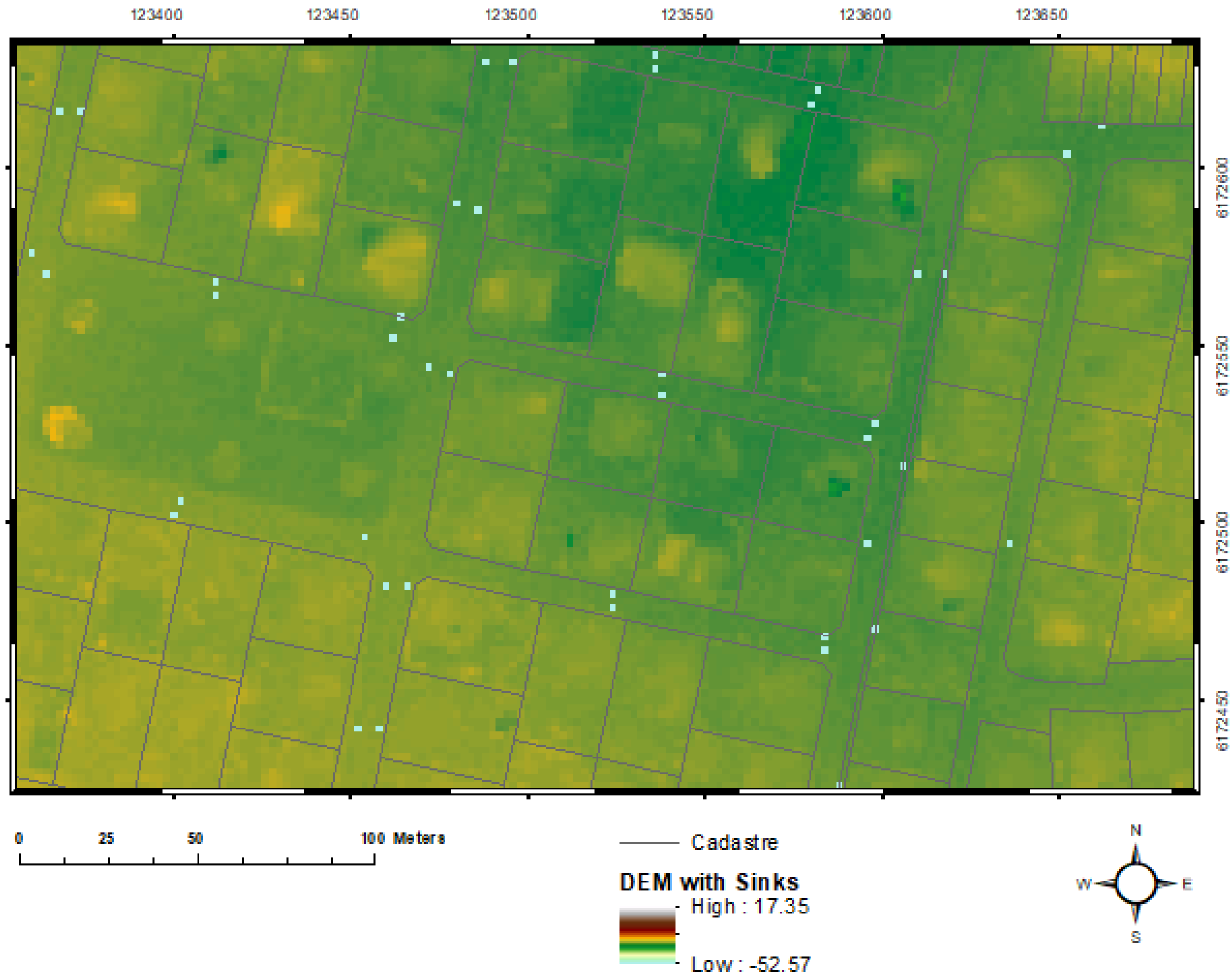

Figure 18 Detail showing sink structures zoomed in (Light blue dots) and cadastre (white lines).

Once sink structures are created then spurious sinks present in the DEM were filled. The created sink structures however were not filled because they are considered as real sinks. This was done by specifying a threshold value of 5 meters. **Figure 19** shows the output HydroDEM generated from DEM having sink cells representing street inlets in the study area. The next steps to build walls and fill the areas bound by the walls are the same as that of D8 method and therefore will be skipped here.

Figure 19 HydroDEM with sink cells unfilled and elevation of buildings raised during DEM pre-processing step. Walls were created around the building polygons and the area bound by the walls was filled in Arc Hydro Tools. This output was converted to ASCII format in order to use it as input DEM to run TFM algorithm in Matlab.

4.2.2 Flow direction

Once HydroDEM is created for both methods, the next step is to use it as input for flow direction assignment. in D8 method flow direction assignment was performed in ArcHydro tools. The output flow direction raster is presented in **Figure 20** below and it was used as input to calculate flow accumulation. In TFM method, flow direction and flow accumulation were computed in Matlab.

To do this, the HydroDEM has to be converted into ASCI format (conversion tools/ArcMap). The output ASCII raster is then used as input to run TFM algorithm in Matlab software. Flow direction output generated from TFM algorithm in Matlab is a result of 8 matrix (8 files) showing drainage paths from each cell to 8 possible directions.

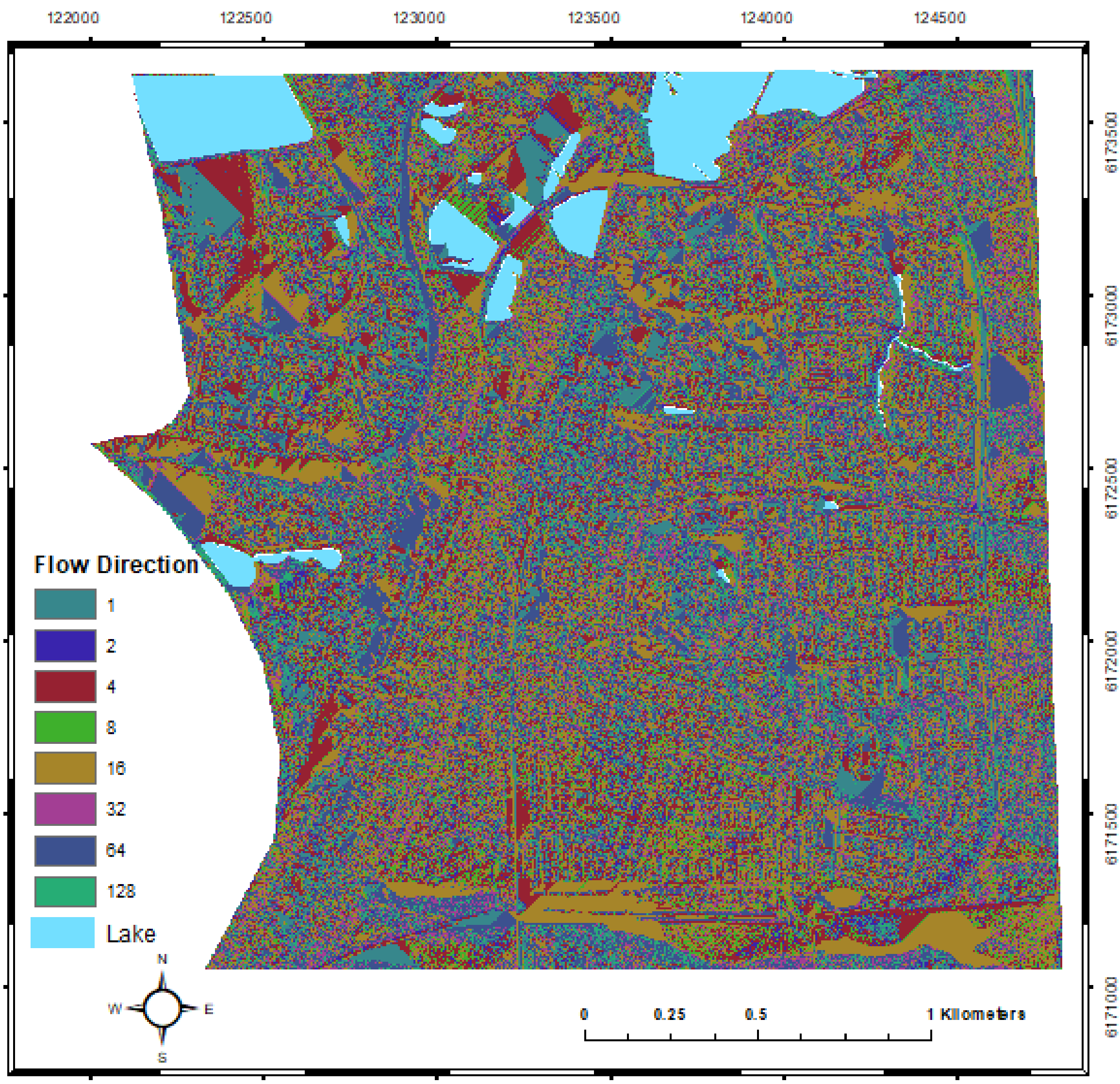

Figure 20 Flow direction raster generated by Deterministic eight-nodes (D8) flow routing algorithm in Arc Hydro Tools.

4.2.3 Preparation of weighted raster

Two different approaches were used to prepare weight raster in D8 and TFM methods as follows. In D8 method, first sub-watersheds were delineated using street inlets as pour points and flow direction raster as an input in ArcMap as shown in **Figure 21**. To visualize the sub-watershed polygons with more detail **Figure 22** was prepared by zooming in some part of the study area.

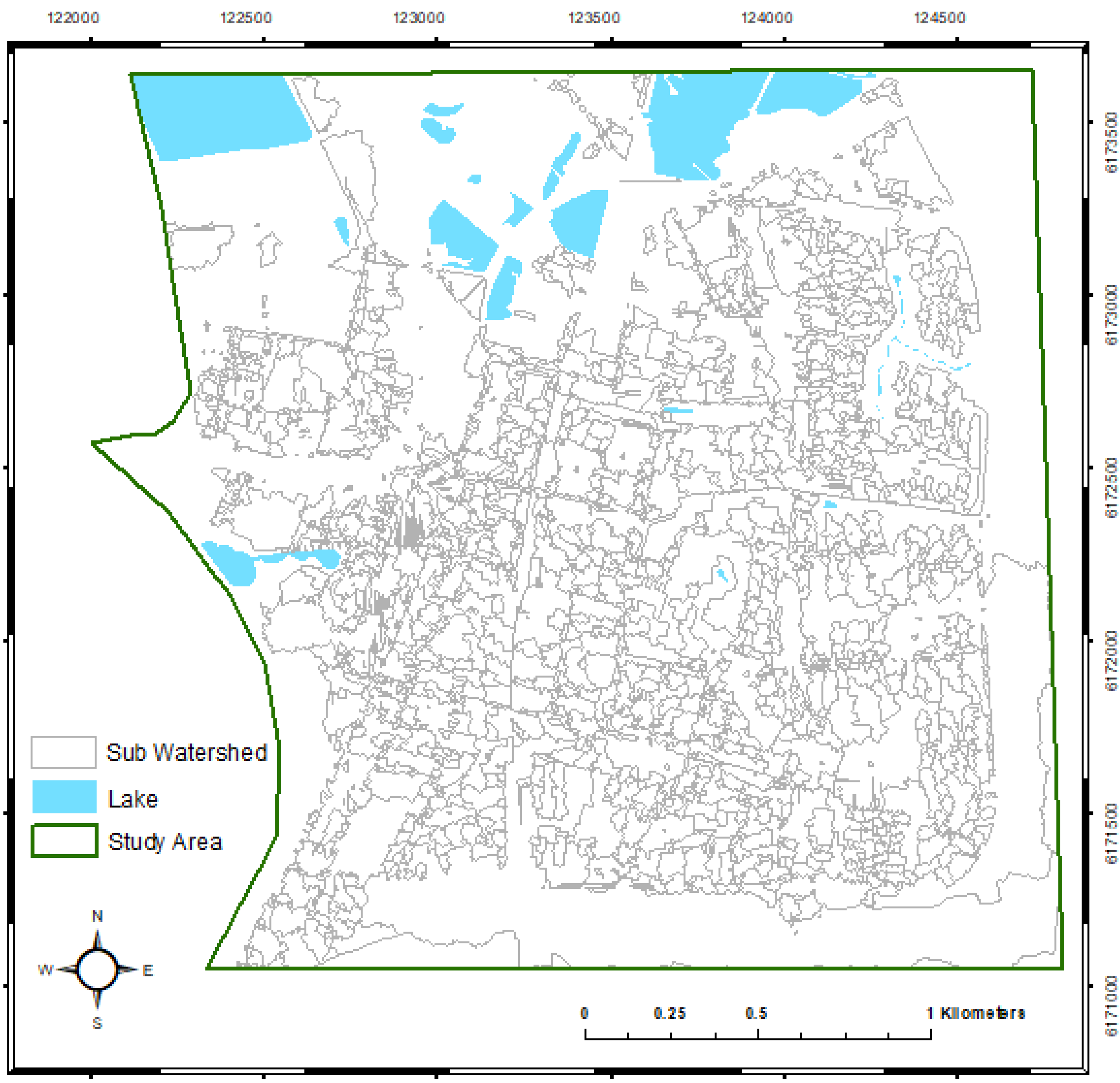

Figure 21 Sub-watershed polygons (Black lines) contributing flow to each street inlets. Street inlet points were used as input pour points during the process in ArcGIS.

Figure 22 Detail of the study area showing sub-watershed polygons (blue lines) overlaid with Ortho photo, with street inlets as pour points marked in (Red points).

The area of each sub-watershed was computed in the attribute table and volume of flow generated from these sub-catchments was calculated by dividing the sub-catchment area to the area of a single cell which is 4 m^2. Flow consumption capacity of street inlets is calculated as follows. From **Section 4.1** above, flow intercepting capacity per unit time of street inlets was estimated to be **0.035** m^3/sec which is equal to **108** m^3/hr. Calculated 10-year return rainfall is **26** mm or **0.026** m. Multiplying 0.026 m by the area of a single cell (4m^2) results **0.104** m^3. This represents volume of water that will be accumulated a single cell during a rainfall of 1-hour duration and 10-year return period. Furthermore, dividing 108 m^3 by 0.104 m^3 is **1038**, which represents accumulated flow in cell units that is equal to the capacity street inlet to intercept flow in an hour. Thus, 1038 cell units is reduced from flow accumulation generated by all sub-watersheds.

After reduction the result can be either of the following (1) If result is positive, then it indicates that the inlet which is located in that sub-watershed has a flow interception capacity less that the accumulated flow to it therefore it will flood. All cells within the sub-watershed will have a weight value which is equal to a proportion of water to be removed to the total volume of water accumulated from the sub-watershed. The excess water continues to flow as surface runoff downslope until it reaches another inlet downstream. (2) If the result is negative value or zero, then it indicates that the draining capacity of the inlet is higher than or equal to the accumulated flow from its sub-watershed. Therefore, all flow accumulated to the inlet will be totally consumed by it, and no runoff will be generated from that sub-watershed. All cells within such sub-watershed will get a weight value of zero. The field that contains the calculated weight values in the sub-watershed polygons layer was then rasterized. The output raster contains Nodata values. These are cells which do not flow to any of the delineated sub-watersheds. Flow from these cells do not reach any of the street inlets thus it will not be intercepted. Due to this reason, these cells are assigned a weight value of 1. The resulted weighted raster showing weight values of cells is presented in **Figure 23** below.

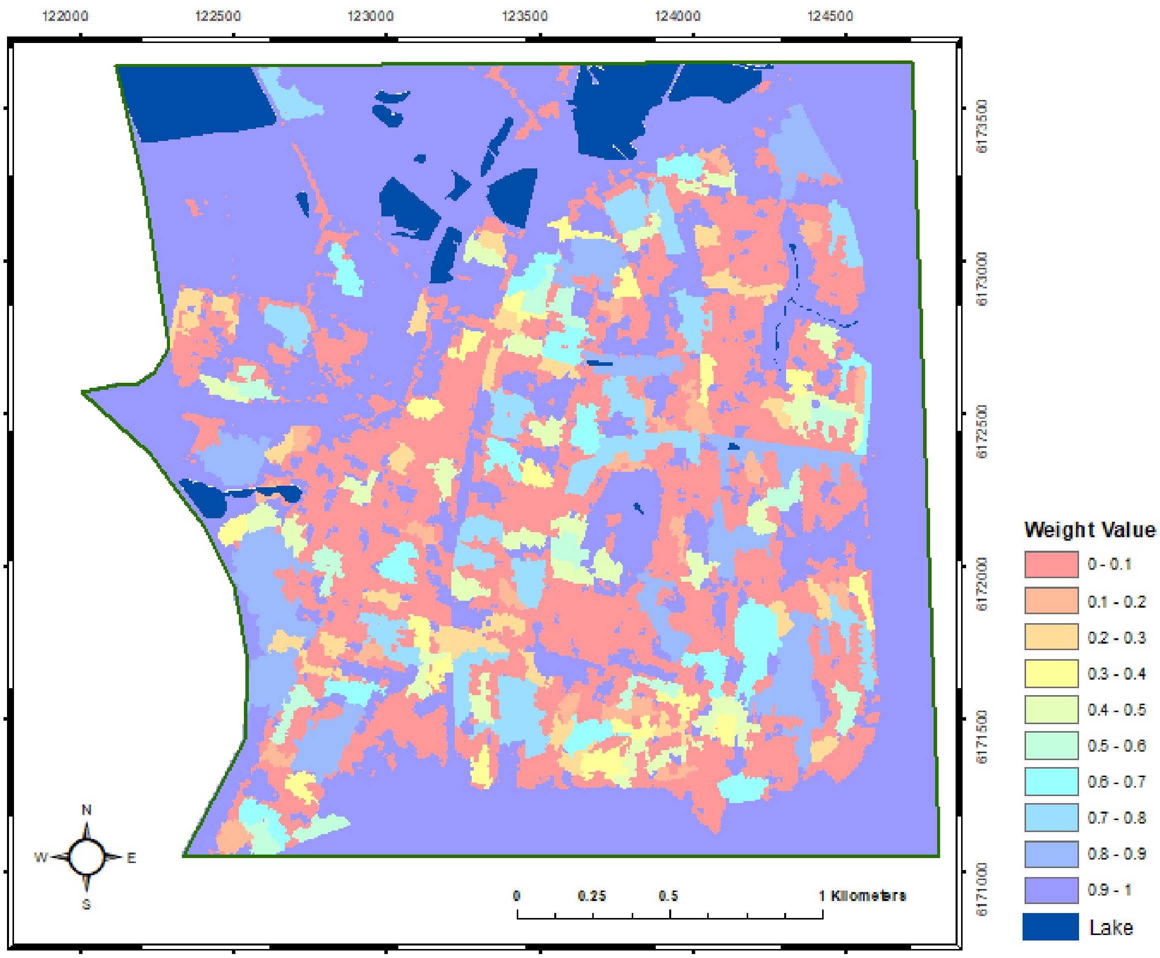

Figure 23 Output weight raster with weight values ranging from 0 – 1. Cells that do not belong to a sub-watershed have a weight value of 1 and all cells within a sub-watershed have the same weight value. It is used as input weight to calculate flow accumulation calculation with inlets trapping effect.

In TFM method, flow accumulation values at sinks cells were extracted and used to prepare weight raster (Spatial Analyst tools). To do this, polygons created by 1-meter buffer around street inlet points were used as input zones and maximum value statistical type was selected for this operation. In the next step, flow interception capacity of street inlets (1038 cell units) was reduced from the extracted flow accumulation values at sink cells. The field containing result of this operation was rasterized and used as weight raster for later use as input to run weighted flow accumulation. **Figure 24** shows weight raster developed in TFM method.

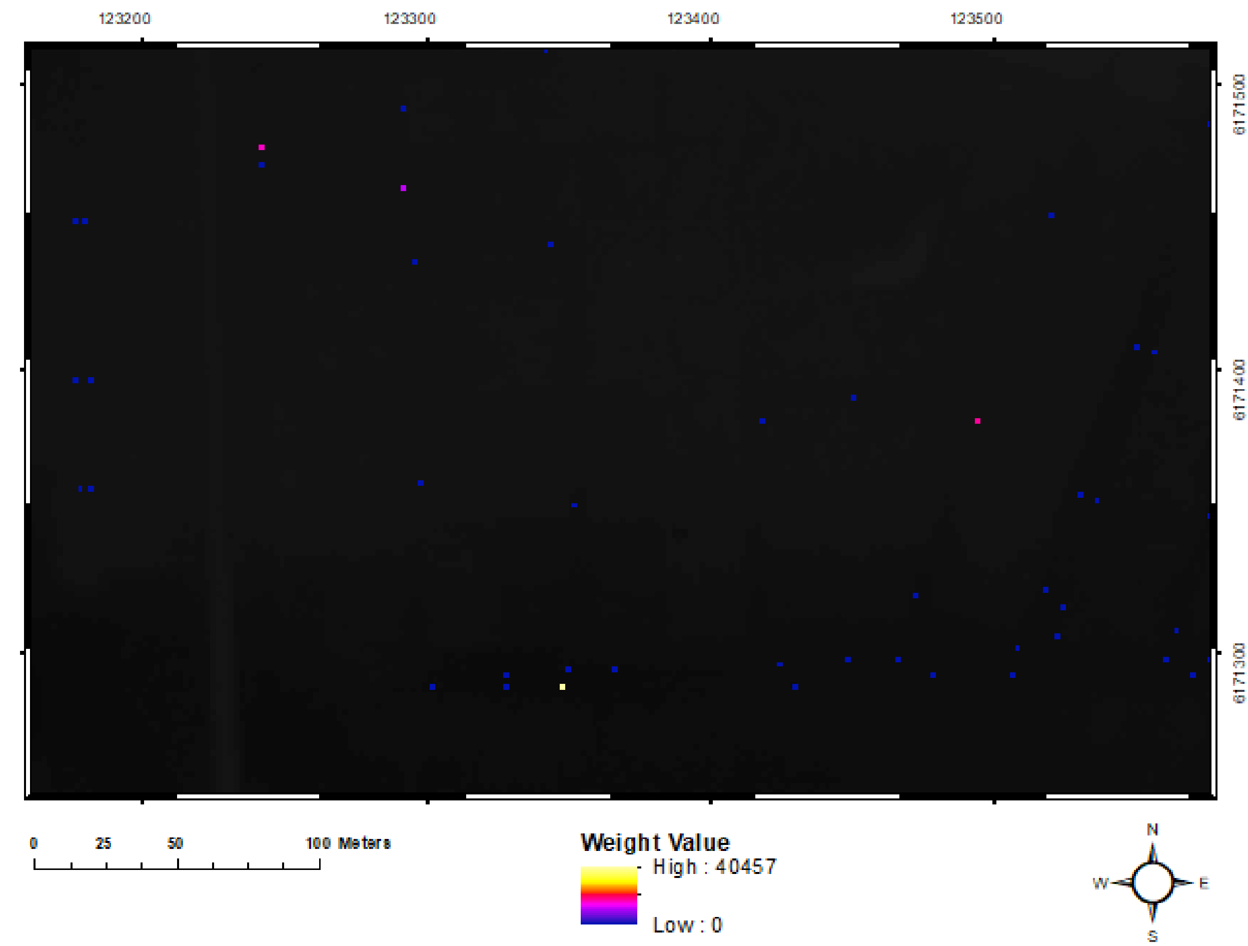

Figure 24 Weight raster created by extracting flow accumulation values at sink cells using Zonal Statistics tool in ArcGIS.

5. Results

In this section flow accumulation results with and without the effect of inlets flow interception is included in the analysis is presented for both D8 and TFM methods. The unit of flow accumulation values is converted from cell units into cubic meters. This was done by multiplying each flow accumulation output having value in cell units by the amount of water in cubic meters that is accumulated in a single cell which is **0.104 m^3** (Ref **Section 4.2.3**). In addition, excess overland flow as well as number and location of street inlets identified with flooding incident from both methods is also presented in this section.

5.1 D8 method

5.1.1 Flow accumulation results without street inlets trapping effect

Flow accumulation calculation was performed in Arc Hydro tools as shown in **Figure 25**. The maximum and minimum flow accumulated value is 550490 and 0 cell units respectively. In D8 method cells that do not have any upstream cells draining into them are assigned zero flow accumulation. However, in reality these cells receive water from the rain and they accumulate flow of 1 cell unit and contribute this flow by draining to cell downstream therefore it has to be accounted in the analysis. To do this, flow accumulation was calculated from the area of each sub-watersheds in the attribute table of the sub-watersheds by dividing the area of sub-watershed to area of a single cell. The output flow accumulation is presented in **Figure 26**, maximum and minimum accumulated flow from sub-watershed is 118373 and 1 respectively.

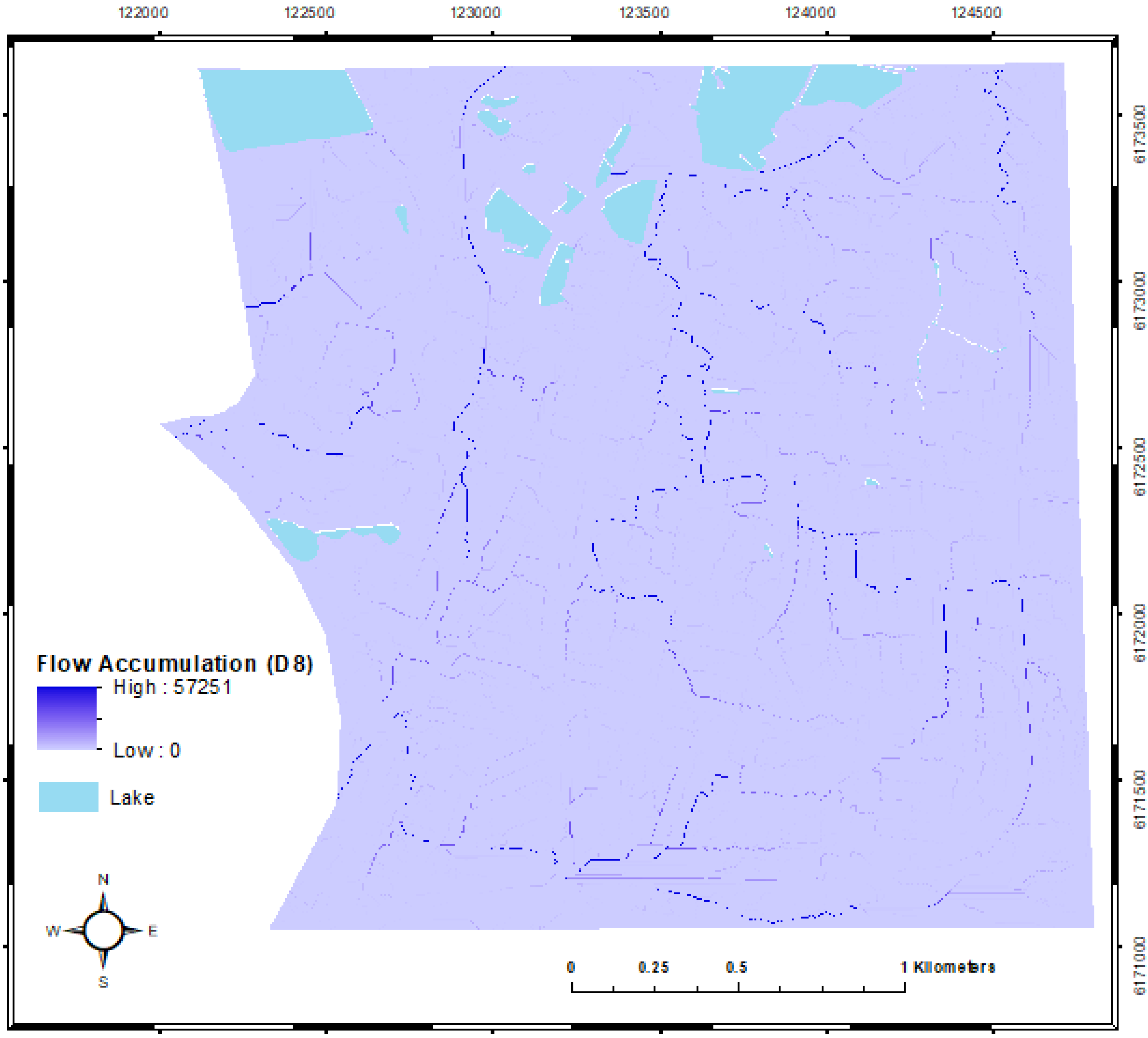

Figure 25 Flow accumulation before street inlets flow interception effect is include in the analysis.

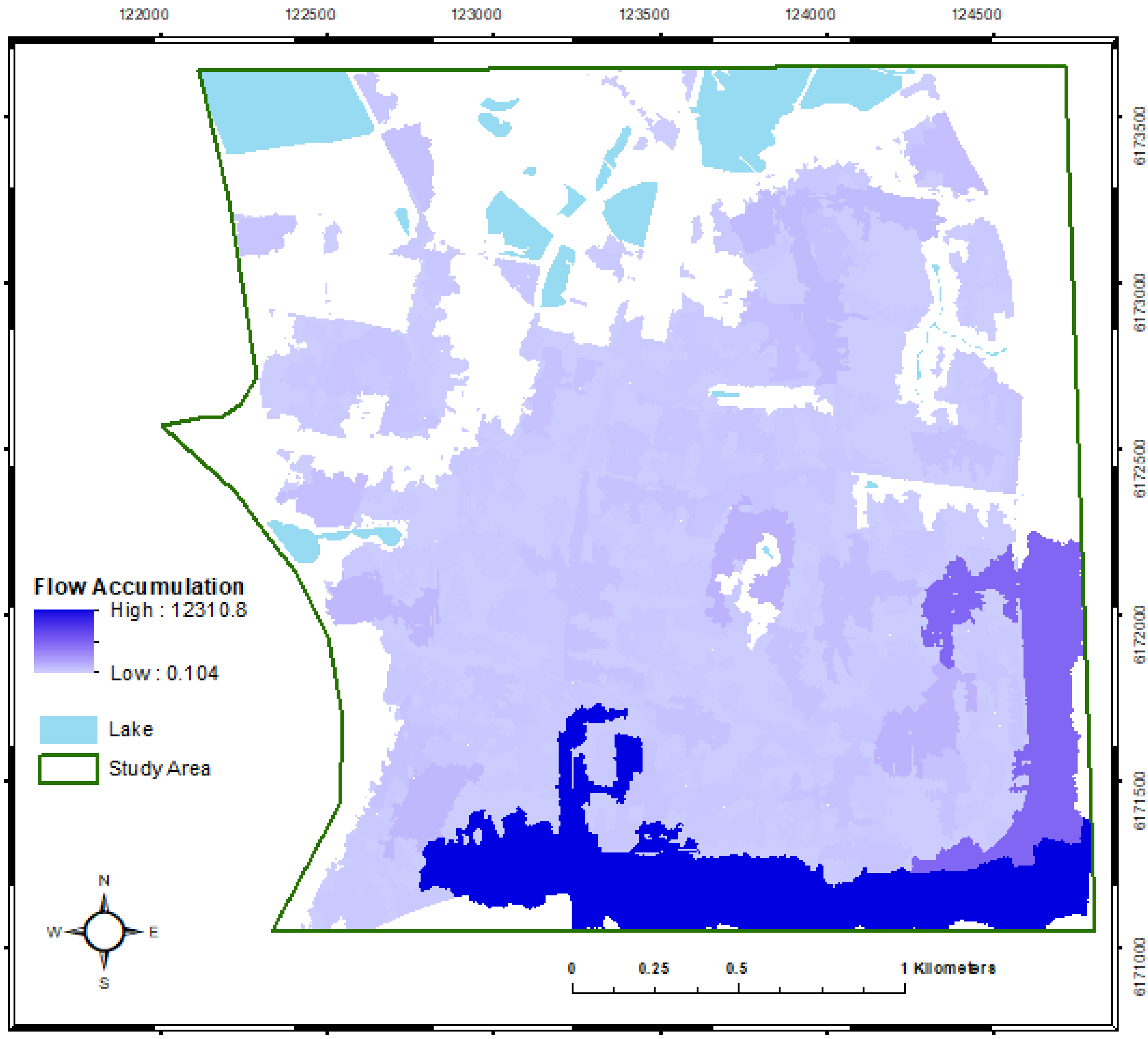

Figure 26 Flow accumulation generated from sub-watersheds in Deterministic eight-nodes (D8) method. Flow accumulation is calculated by dividing the area of sub-watershed to the area of a cell in the DEM.

5.1.2 Flow accumulation result with street inlets trapping effect

Flow accumulation with weight was performed using Flow Accumulation tool in ArcMap and the weight raster prepared in **Section 4.2.3** and flow direction prepared in **Section 4.2.2** as input. Result of the step is presented in **Figure 27**.

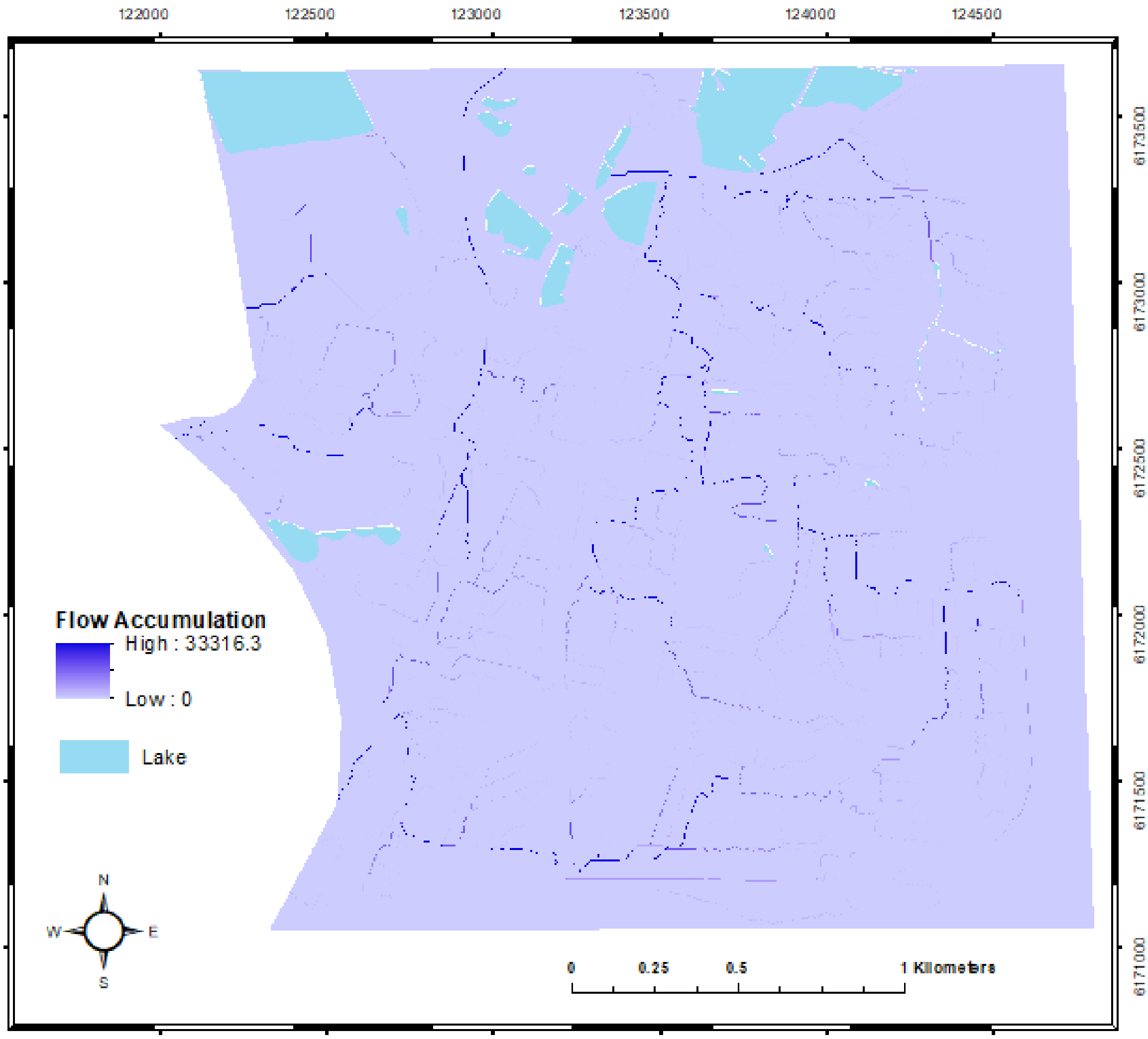

Figure 27 Flow accumulation result with street inlets flow interception effect (Weighted flow accumulation). Flow direction and weight raster generated in Figure 20 and 23 respectively were used as inputs.

5.2 TFM method

5.2.1 Flow accumulation result without street inlets trapping effect

Flow accumulation result generated using TFM algorithm from 8 triangular facets constructed by the algorithm is presented in **Figure 28.** In order to calculate flow accumulation from a 2m X 2m cells, the output was divided by 8. The output of this operation is presented in **Figure 29.**

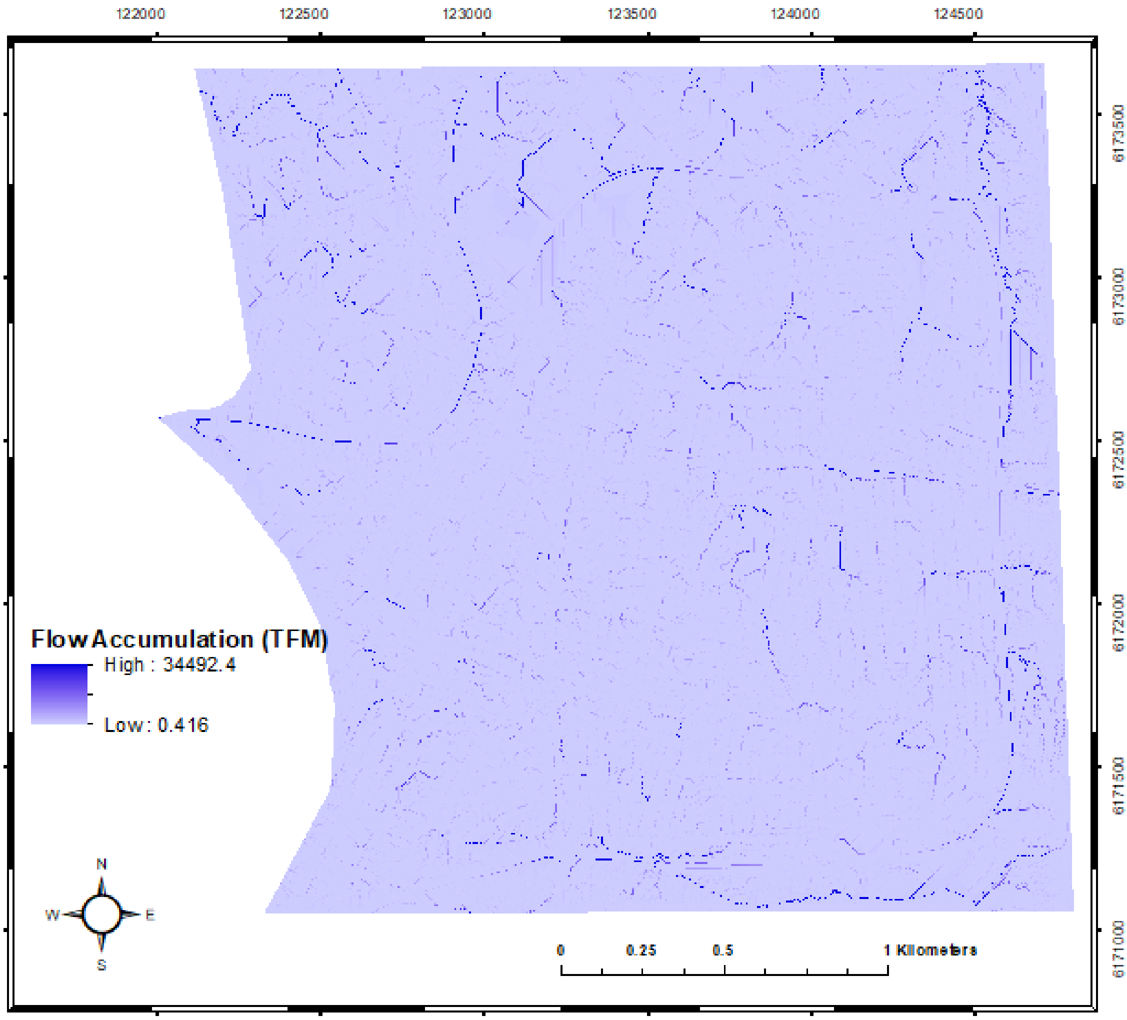

Figure 28 Flow accumulation result calculated by running TFM algorithm in Matlab. The effect of street inlets flow interception is not included. The values represent accumulation of flow from the triangular facets created by the algorithm.

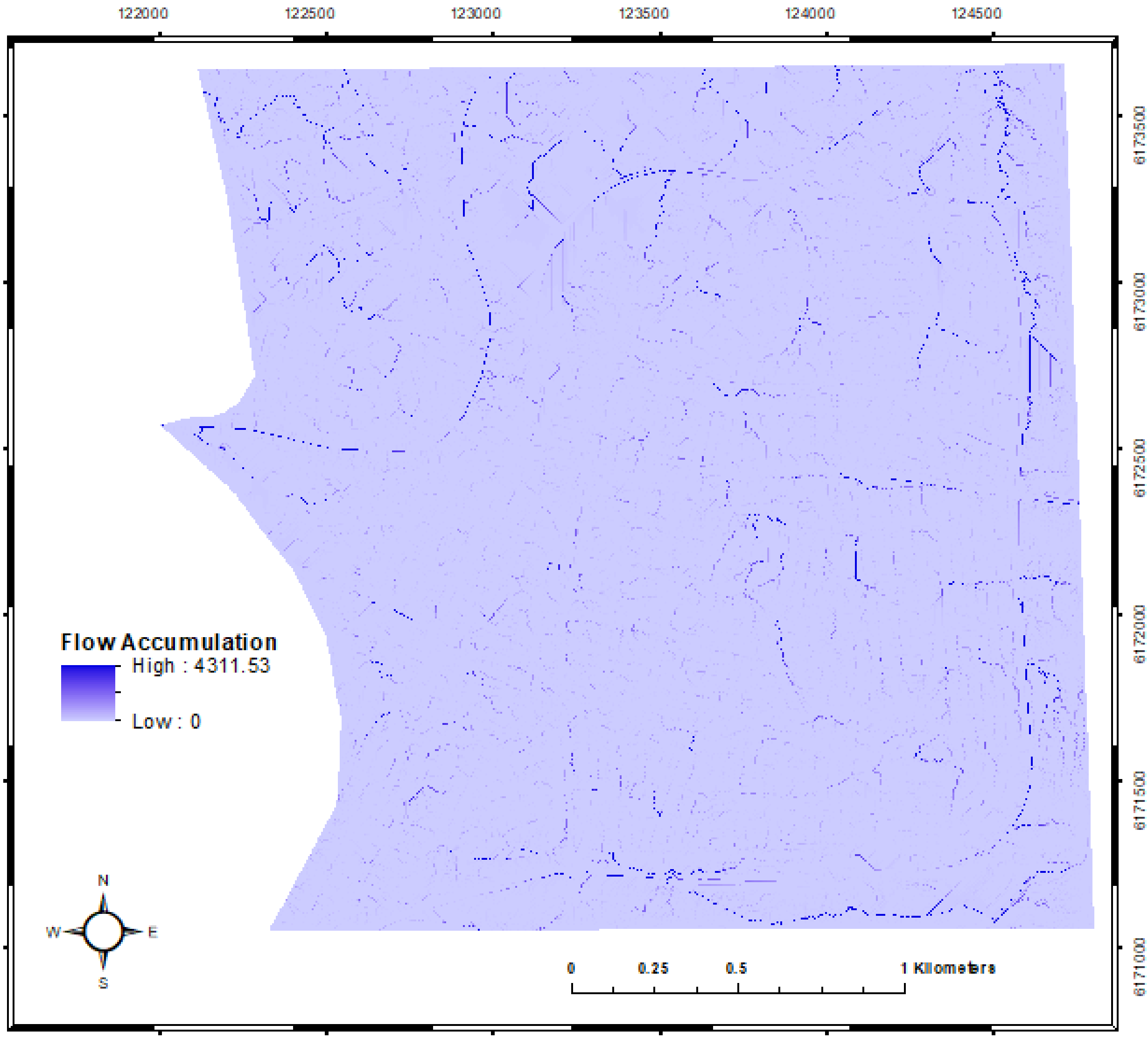

Figure 29 Flow accumulation result from 2m X 2m cell size calculated by dividing the flow accumulation output in Figure 28 above by 8.

5.2.2 Flow accumulation result with street inlets trapping effect

In TFM method calculation of flow accumulation with weight was performed with a different tool. The tool was developed by Dilts (2015) and it can be added to the Arc Toolbox / ArcGIS. **Figure 30** below shows weighted flow accumulation result that was generated after street inlet's flow interception is taken into account.

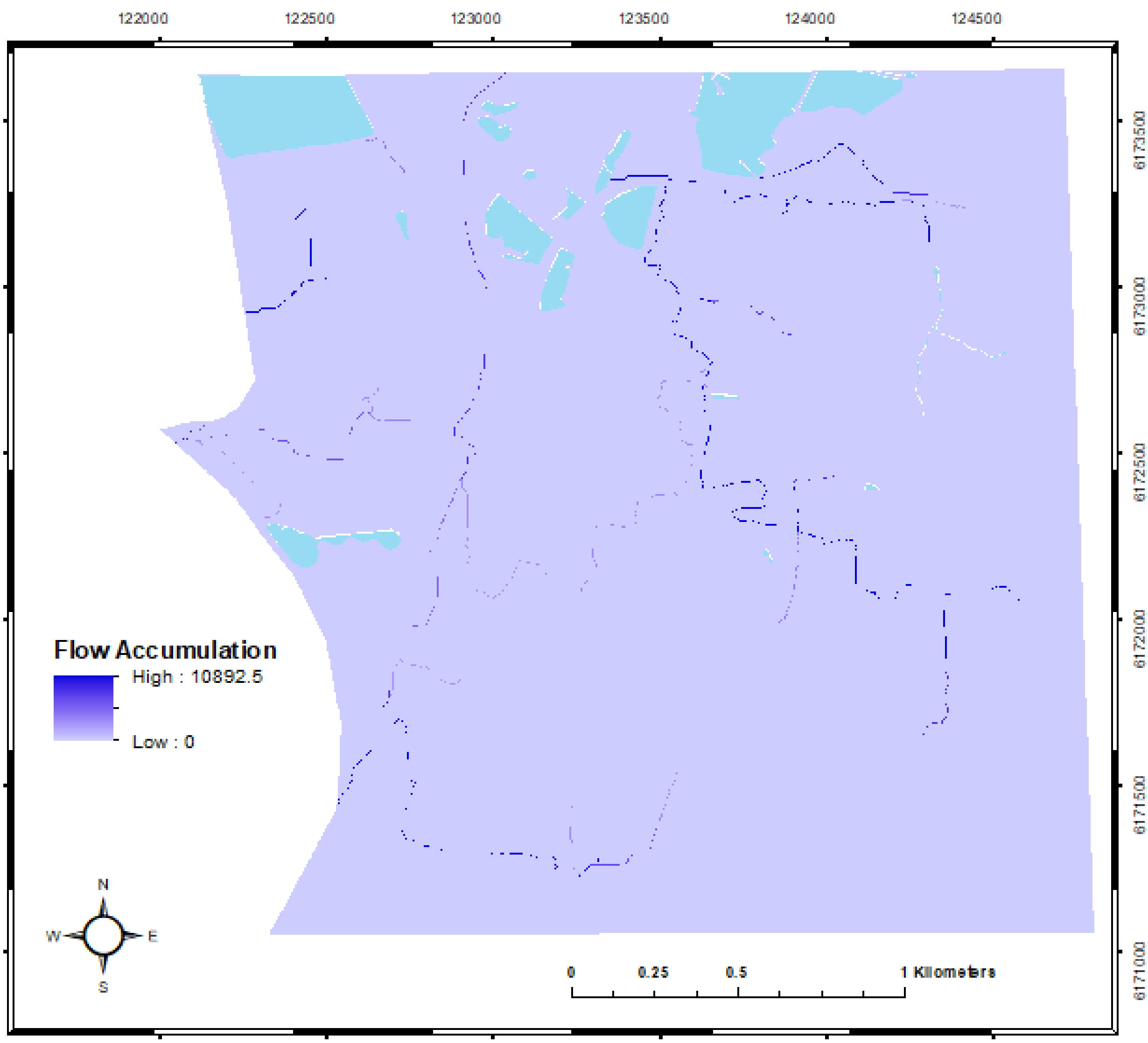

Figure 30 Flow accumulation result with street inlets flow interception effect (weighted flow accumulation). Flow direction and weight raster in Figure 20 and 24 respectively were used as inputs.

5.3 Flooding incident at location of street inlets

The locations of street inlets where flooding is expected to occur were identified from the weighted flow accumulation raster outputs of both D8 and TFM methods. To do this, once the amount of flow that is consumed by street inlets is reduce then standard query language (SQL) was used.

In D8 method, flow interception capacity of street inlets is subtracted from flow accumulation generated by each sub-watershed. After the reduction all positive results were selected using SQL. Positive result after reduction indicate flooding because it tells that inlet which corresponds to that sub-watershed has flow interception capacity that is lower than the flow accumulated to it.

In TFM method, since flow accumulation is calculated at sink cells that represent the street inlets, the reduction is directly from the extracted flow accumulation values at sink cell. The identified number of flooded inlets in D8 and TFM methods is 202 and 80 respectively. The total number of street inlets included in the analysis of this study is 2338. **Figure 31** and **Figure 32** below show the location of all street inlets with potential flooding incidents for D8 and TFM methods respectively.

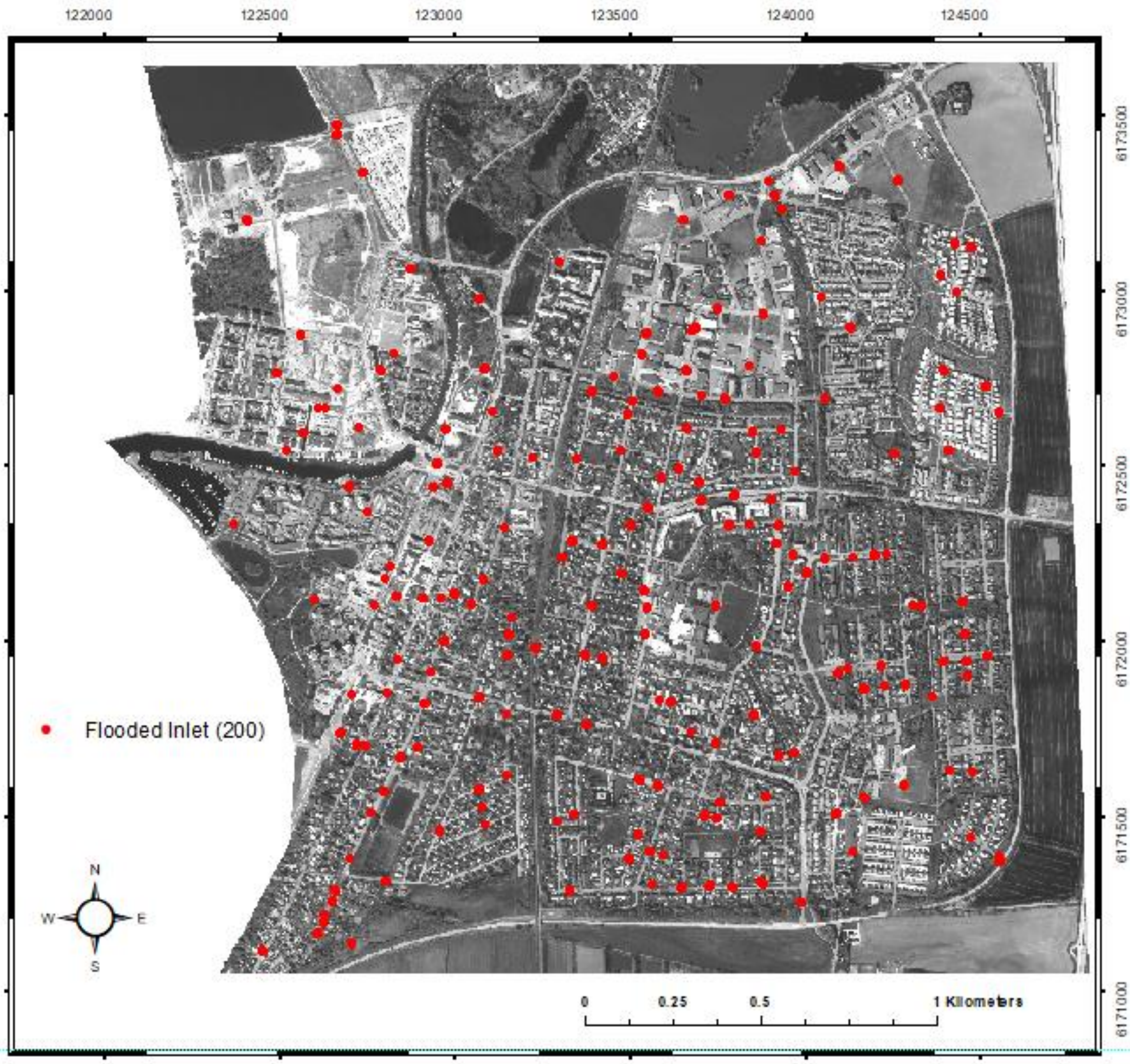

Figure 31 Location of flooding incident at 202 street inlets (Red points) overlaid with Ortho photo in Deterministic eight-nodes (D8) method.

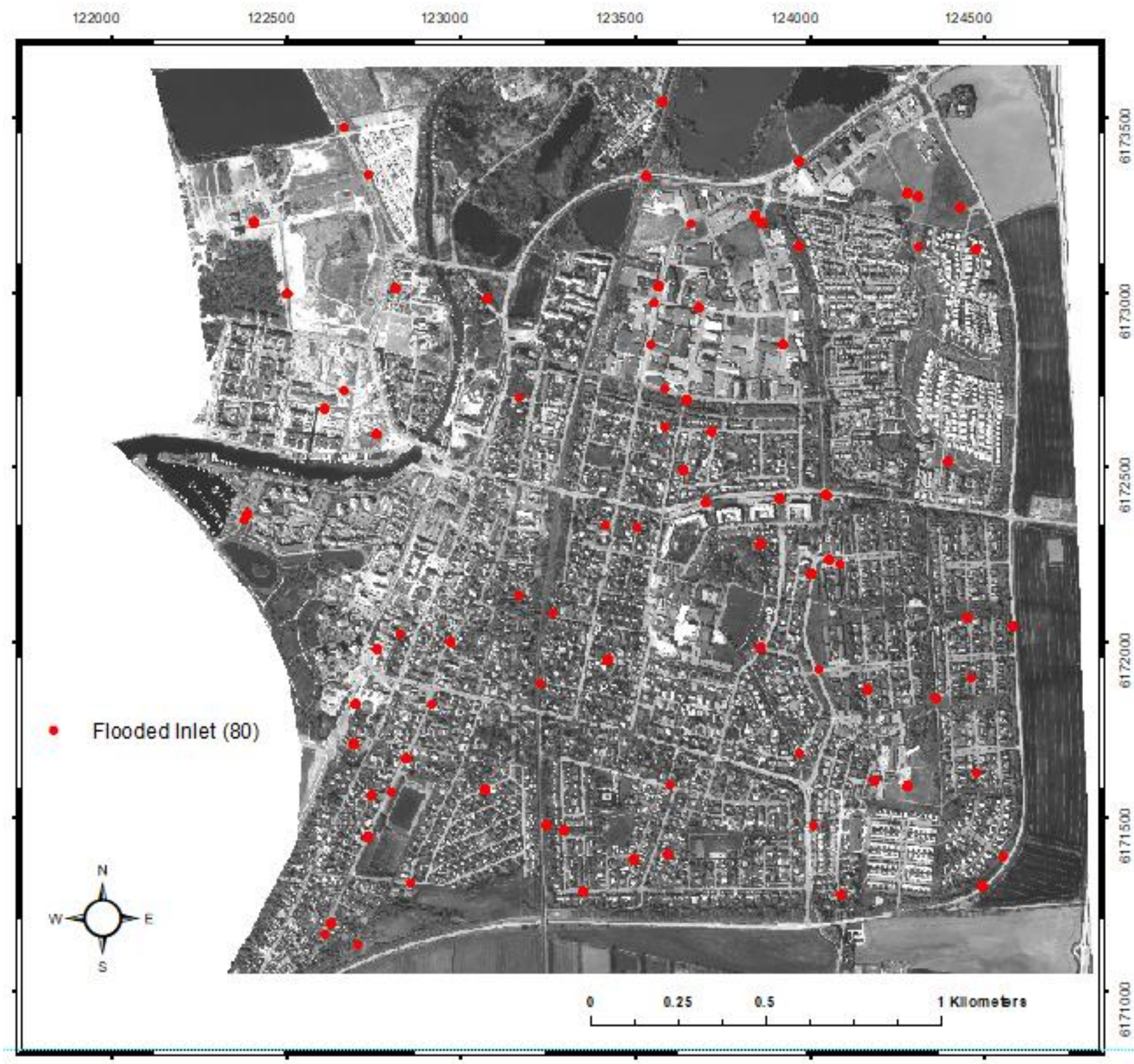

Figure 32 Location of flooding incident at 80 street inlets (Red points) overlaid with Ortho photo in Triangular Form based Multiple Flow Direction (TFM) method.

5.4 Excess overland flow path inside the study area

To extract excess overland flow path, a threshold value of 5000 was specified in both methods. In other words, streams having flow accumulation value of 5000 or less are considered as low potential to cause significant flooding, therefore were ignored during the overland flow path extraction process. **Figure 33** and **Figure 34** below show excess overland flow above the threshold value generated from D8 and TFM method respectively.

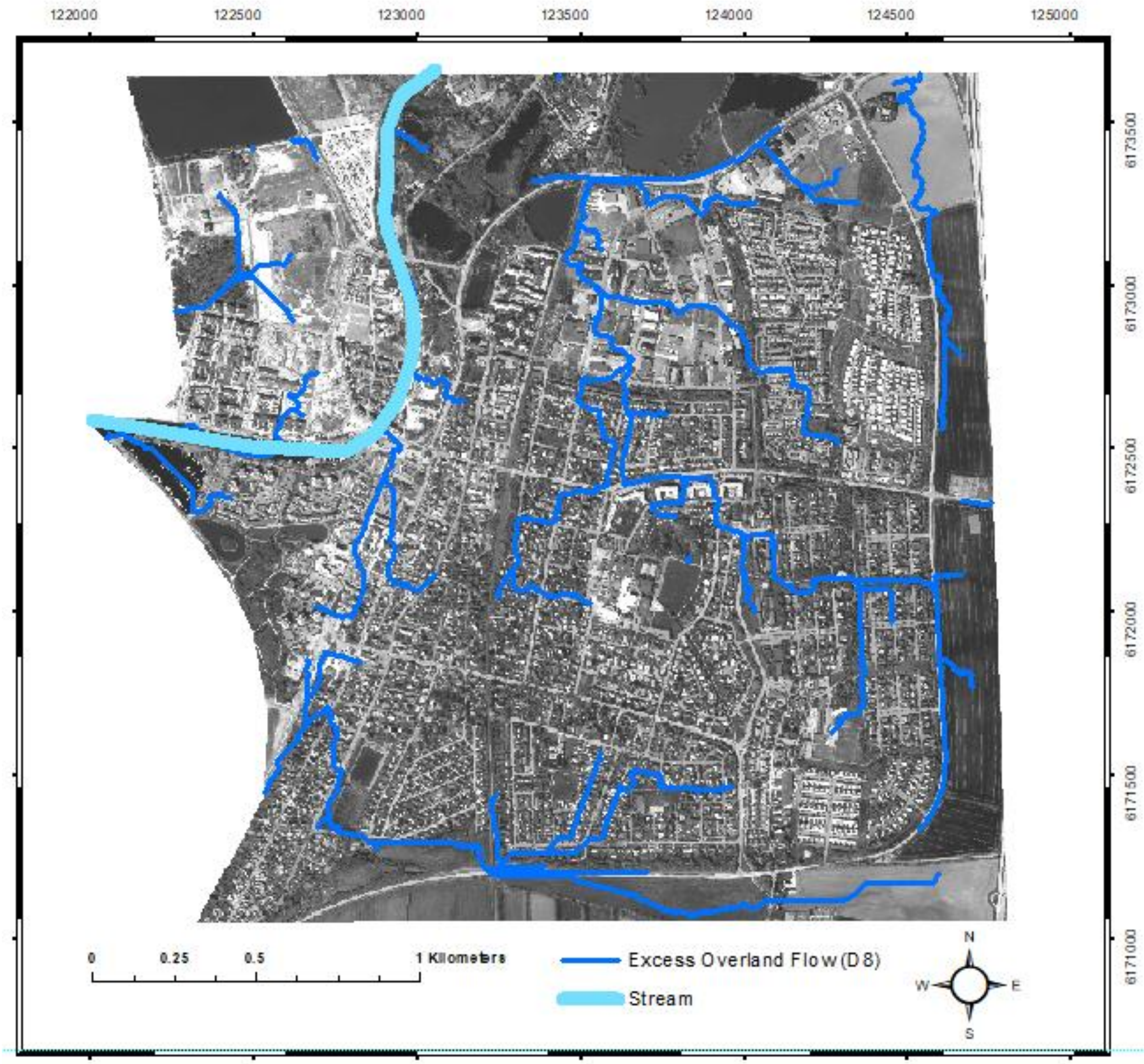

Figure 33 Excess overland flow path in the study area generated by Deterministic eight-nodes (D8) method. The blue lines represent excess flow when a threshold value of 5000 is used.

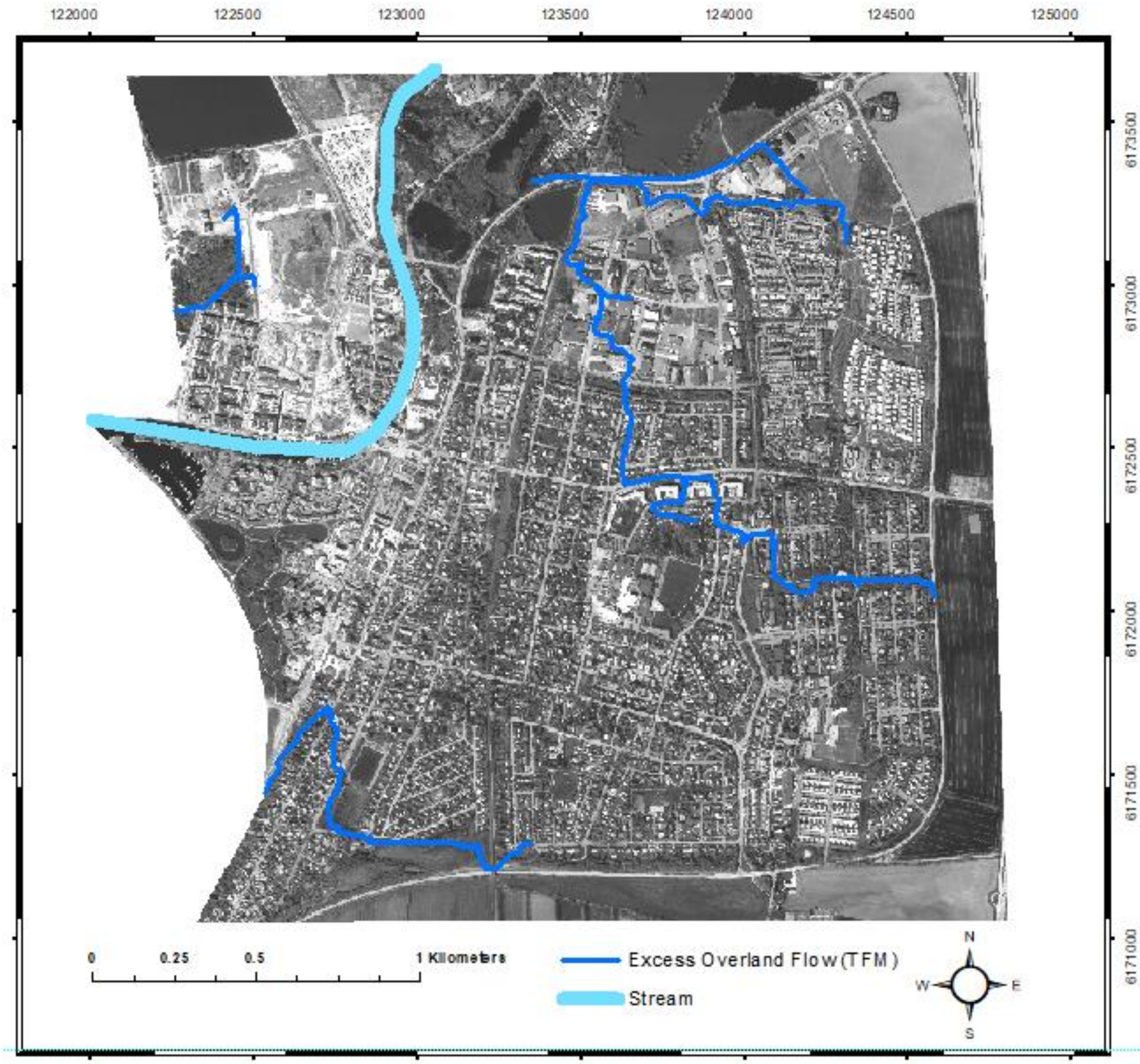

Figure 34 Excess overland flow path generated by Triangular Form based Multiple Flow Direction (TFM) method. The result shows less excess flow path compared to excess overland flow resulted from Deterministic eight-nodes (D8) method in Figure 33 above using the same threshold value (5000).

6. Discussion

6.1 Summary of results from D8 and TFM methods

Summary of the results derived by D8 and TFM methods is presented in **Table 3**.

Table 3 Showing summary of results on flow accumulation (with and without inlets flow trapping effect) and the number of identified flooding incidents at street inlets that are generated when Deterministic eight-nodes (D8) and Triangular Form based Multiple Flow Direction (TFM) algorisms are used as a flow routing methods on the DEM.

Result	**D8 method**		**TFM method**	
	No inlet trap effect	With inlet trap effect	No inlet's trap effect	With inlet trap effect
Flow accumulation from the whole catchment (m^3)	**57,271**	**33,316**	**45,028**	**10,893**
Max accumulated flow in a street inlet (m^3)	**12,311**		**4,311**	
Flooded street inlets	**202**		**80**	

Although the study area's coverage, input data used, precipitation data (10-year return rainfall) and the model assumptions described in **Section 4.1** are the same in D8 and TFM methods, the results generated by the two models are different as shown in the summary **Table 3** above. Maximum flow accumulation value before including the flow that is intercepted by street inlets into the analysis is 52,271 m^3 and 45,028 m^3 in D8 and TFM methods respectively. This difference is due to the two algorithms ability to represent dispersion of overland flow on the terrain slope. Explained further, D8 algorithm is non dispersive i.e. each grid cell in the DEM contributes 100% of its accumulated flow to only one downstream neighbouring cell. TFM algorithm on the other hand is dispersive and each grid cell in TFM algorithm is divided into 8 triangular facet as mentioned in **Section 2.5.2**. Depending on the direction of flow assigned to the facets, the water contained in them is directed to more than one adjacent cells that can terminate in different outlets entirely. Especially those facets which are located at a boundary of sub-watersheds can be directed to the two adjacent sub-watersheds. Due to this, flow accumulation values at sink cells that can be generated fb yD8 and TFM method is different. Accordingly, the number of street inlets with potential flooding incident identified by the two methods is also affected which is 202 and 80 flooded inlets in D8 and TFM methods respectively.

Flow accumulation values with inlets trapping effect included in the analysis is 33,316 m^3 and 10,893 m^3 for D8 and TFM respectively. According to experiment made in a published research by Petter and Hasan. ‘’A Triangular Form Based Algorithm to Estimate Overland Flow Distribution and Accumulation on a Digital Elevation Model.’’ *Transaction in GIS* 18(1) (2014): 108-124, TFM algorithm generates more accurate results of overland flow distribution and accumulation compared to other eight algorithms including D8 algorithm. Based on the conclusion of their research, it is suggested that the results generated by TFM method in this study are considered more reliable than that of D8 method. However, important assumptions were made in **Section 4.1** regarding processes such as infiltration and other forms of losses like evaporation and interception. In this study the three processes are assumed to be zero. Considering the duration of rainfall used for analysis in this study which is 1-hour, evaporation and interception are insignificant. However, infiltration loss is important and might significantly affect the results depending on area coverage in percentage of pervious and impervious surfaces in the area, thus it is interesting to quantify and include infiltration parameter in the analysis in order to investigate more accurately whether the existing drainage system in the study area has satisfactory conveyance capacity. To do this, soil analysis and land use classification needs to be performed and once infiltration loss is quantified then it can be incorporated into the weight raster preparation described in **Section 4.2.3**. Excess overland flow extraction is done based on a flow accumulation threshold value which is determined by the user. In this study threshold value 5000 for excess overland flow path extraction. Therefore, flow accumulation value above the threshold value is considered as flow that has a potential of generating a significant flooding.

6.2 Effect of building walls on flow direction and flow accumulation results

The key parameter when performing urban flood modelling is flow direction. This is why it is very essential to pre-process the DEM before extracting flow direction from it. Flow direction assignment and flow accumulation calculation extracted before raising elevation of buildings by creating walls at boundaries of building polygon is as shown in **Figure 35** below. It can be seen from the figure that streams (blue lines) crossing the buildings (red lines). This overland flow path does not represent reality. However, after building walls around the building polygons and filling the area bound by the walls in Arc Hydro tools, the derived flow direction and overland flow path become realistic as shown in **Figure 36.**

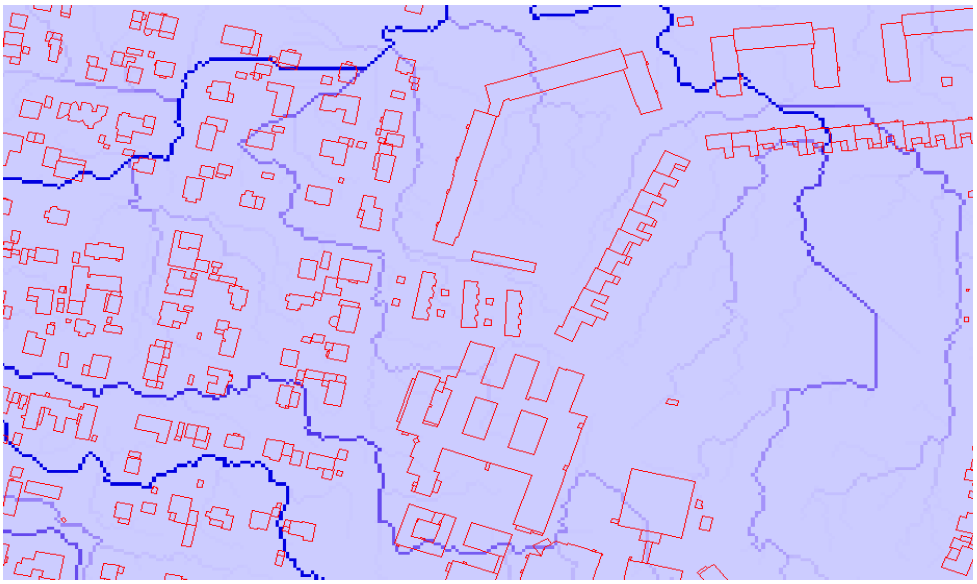

Figure 35 Illustration of incorrect stream network path (blue lines). The streams are crossing the buildings (Red polygons) due to the absence of elevation of building on the DEM that is used to generate HydroDEM and flow direction assignment.

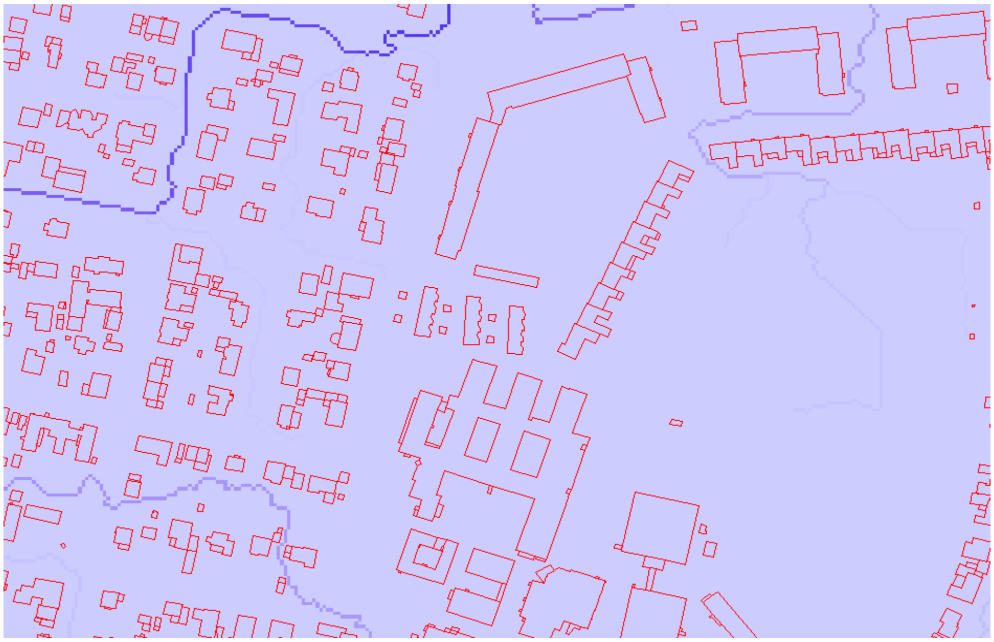

Figure 36 Illustration of corrected overland flow path (blue lines). Elevation of buildings was modified on the DEM during DEM pre-processing steps using Arc Hydro Tools. HydroDEM generation and flow accumulation calculation was based on the modified DEM.

6.3 The main challenges faced during development of the models

In this section the challenges that were faced during the development of D8 and TFM method will be explained.

The main challenge in D8 method is related to the limitation of the flow accumulation tool in ArcGIS. The tool works only when cells have positive values and it treats negative values as zero by default. Therefore, the reduction of losses such as flow consumption by street inlets by assigning negative weight value is impossible. To overcome this challenge, a portion of the water received by each cell is reduced so that the cumulative water reduced from all the cells inside a particular sub-water is equal to the flow interception capacity of its pour point inlet during 1-hour rainfall of 10-year return period. This was done by assigning the cells a weight value ranging between 0 – 1 as explained in **Section 4.2.3.**

The challenge faced in TFM method is due to (1) flow direction output that is derived by running TFM algorithm is matrix of 8 files (not a single raster), which cannot be used as input to run weight flow accumulation (2) sub-watershed areas delineation using all of the street inlets as pour points cannot be performed in TFM algorithm. It is obvious that with the lack of these two inputs, flow accumulation tool in ArcGIS cannot be used as it was done in D8 method. Therefore, a different flow accumulation tool that can accommodate negative values described in **Section 5.2.2** Unlike flow accumulation tool in ArcGIS, this tool allows cell to be assigned negative weight value. However, the limitation of this tool is that when a sink cell receives flow accumulation which is less than its flow interception capacity then the tool assigns the negative difference as accumulated flow to the cell. In this case, since all the flow accumulated into the sink cell will be consumed by the sink cell, the tool should assign zero flow accumulation at these cells instead. The cell which is located downstream of the sink cell will then get flow accumulation from all cells draining to it from other directions. To overcome this, flow accumulation values at sink cells were extracted then inlets flow interception was subtracted. This operation was done in the attribute table of the extracted values. The field containing the result of this operation is then rasterized to be used as weight for sink cells. Other cells in the DEM were assigned a weight value of zero.

6.4 Visual comparison of results with other research.

The key research question in this study is whether a simplified GIS-based urban flood modelling approach produces a reasonable outcome. Thus, the excess overland flow derived by D8 method in this study is visually compared to inundated areas derived from 2D modelling using HEC-RAS model, a research conducted by Betsholtz and Nordlöf. (2017) as shown in **Figure 37**. The location and coverage of the study area is the same in both studies. However, it is important to note that the D8 model developed in this study is a static model and do not include time factor in the analysis. HEC-RAS model on the other hand is dynamic and the result presented below is generated after 2-hour simulation time. With such differences it is not possible to make quantitative comparison of the results of both studies. However, visual observation of inundated areas derived by the two studies show a significant similarity. Especially results derived by 6m (red) computational mesh in HEC-RAS model and excess overland flow derived by D8 method in this study (right). This visual comparison shows simplified GIS-based urban flood modelling approach can produce reasonable result. However, for future investigation using the developed models it is recommended that the limitations of this study be quantified and included in the analysis. The limitation of this study are as listed in the next **Section 6.5** below.

Figure 37 Visual comparison of flood inundated areas by D8 method in this study (right) and HEC-RAS model (left) after 2 hours of simulation (Source: Betsholtz and Nordlöf, 2017).

6.5 Limitations

There are two key limitations encountered in this study

- Due to the lack of information regarding the actual capacity of street inlets it has to be estimated as described in **Section 5**.
- Infiltration and other forms of losses are assumed to be zero, thus were not included in the analysis.

7. Conclusions and Recommendations.

In this research two simplified GIS-based flood models were developed to perform flood modelling in Lomma. The models were developed using two different flow direction algorithms namely, the SFD deterministic eight-node algorithm (D8) and the MFD Triangular Form Based Multiple Flow Algorithm (TFM). Visual comparison of inundation extent derived in this study with other researches for the same study area shows that the models developed in this study can produce reasonable outcomes. The results show that excess flow accumulation generated (after street inlets interception capacity is include in the analysis) is 33,316 $m^3$and 10,893 m^3 using D8 and TFM method respectively. Flooding incident at location of street inlets is 202 and 80 inlets in D8 and TFM method respectively. This difference is explained by the two algorithms ability to represent dispersion of overland flow on the terrain slope. TFM algorithm represents overland flow more accurately than D8 algorithm. This is because TFM algorithm divides a cell into 8 triangular facets and models movement of water within a cell before distributing it to one or more of the eight neighbouring cells. Thus, the model developed using TFM algorithm is considered to be more reliable. This study also shows the results that can be generated from GIS-based approach urban flood modelling are different depending on whether single flow direction algorithm D8 or multiple flow algorithm TFM is used to estimate overland flow distribution and flow accumulation of the area under investigation. Assuming infiltration and other form of losses to be zero, the results indicated inundation in some part of the area, however it is recommended that infiltration loss is quantified and included in the analysis before a conclusion can be made regarding the existing drainage system capacity to covey a 10-year return rainfall event of 1-hour duration.

References

Aksoy, H., Kirca, V. S. O., Burgan, H. I. & Kellecioglu, D., 2016. Hydrological and hydraulic models for determination of flood-prone and flood inundation areas. *Proceedings of the International Association of Hydrological Sciences,* Volume 373, pp. 137-141.

Amarnath, G., Alahacoon, N., Smakhtin, V. & Aggarwal, P., 2017. *Mapping Multiple Climate-related Hazards in South Asia.* IWMI Research Report 170 ed. Colombo, Sri Lanka: International Water Management Institute (IWMI).

Ana, M. M. & Möllers, A., 2006. Urban Sprawl in the Öresund Region. Master thesis (*Blekinge Tekniska Högskola)*

Argue, J., 1986. *Storm drainage design in small urban catchments: a handbook for Australian practice.* Vermont South Victoria: Australian Road Research Board.

Aronoff, S., 1989. *Geographic Information Systems: A management perspective.* Ottawa: WDL.

Bedient & Huber., 1948. Hydrology and Flooding analysis. *Addison Wesley Publishing Co*.

Betsholtz, A. and Nordlöf, B. 2017. *Potentials and limitations 1D, 2D, and coupled 1D-2D flood modelling in HEC-RAS. A case study on Höje river*. MA thesis. Lund University.

Beven, K.J., Moore, I.D. (Eds.), 1993. *Terrain Analysis and Distributed Modelling in Hydrology (Advances in Hydrological Processes)*. Wiley.

Bhavsar, V. & Patel, A., 2015. Peak Flood Probability Analysis for Sabarmati River, Gandhinagar. *International Journal for Scientific Research & Development*, 3(03), pp. 789-792.

Brown, S. et al., 2009. *Urban Drainage Design Manual, Hydraulic Engineering Circular 22.* Third Edition ed. Washington, D.C.: Federal Highway Administration, US Department of Transportation.

Cooper, W., 2013. *Multi-Flow Direction Algorithms in GIS.* [Online] [Accessed 30 June 2017].

Dilley, M. et al., 2005. *Natural Disaster Hotspots: A Global Risk Analysis.* Washington, DC: World Bank.

Dilts, T.E. 2015. *Flow Accumulation for Both Positive and Negative Values Toolbox for ArcGIS 10.1*. University of Nevada Reno. Available at: http://www.arcgis.com/home/item.html?id=40d33968c44e4c9395c9c1ff1edd2bbe

Djokic, D., 2008. *Comprehensive Terrain Preprocessing Using Arc Hydro Tools.* Redmont, California: ESRI.

Djokic, D. & Maidment, D., 1991. Terrain analysis for urban stormwater modelling. *Hydrological Processes,* 5(1), pp. 115-124.

ESRI, 2004. *Arc Hydro Tools Overview.* Redlands, California: ESRI.

ESRI, 2011. *Arc Hydro Geoprocessing Tools – Tutorial Version 2.0.* Redlands, California: ESRI.

Ghosh, S. N., 2014. *Flood control and drainage engineering.* 4th ed. London: CRC Press.

Hutchinson, M. F., 1989. A new procedure for gridding elevation and stream line data with automatic removal of spurious pits. *Journal of Hydrology,* Volume 106, pp. 211-232.

Hutchinson, M. et al., 2008. *GEODATA 9 Second DEM and D8 User Guide,* Canberra: Fenner School of Environment and Society, Australian National University, Geoscience Australia.

http://www.lansstyrelsen.se/skane/En/miljo-och-klimat/Pages/default.aspx

http://opendata-download-metobs.smhi.se/explore/

Jenson, S. K. & Domingue, J., 1988. Extracting topographic structure from digital elevation data for geographic information system analysis. *Photogrammetric Engineering and Remote Sensing,* 54(11), pp. 1593-1600.

Khatami, S. & Khazaei, B., 2014. Benefits of GIS Application in Hydrological Modeling: A Brief Summary. *Journal of Water Management and research,* 70(1), pp. 41-49.

Kunapo, J., Peterson, J. & Chandra, S., 2007. *Spatial data integration for accurate parcel level sub-catchment delineation for hydrological modelling.* Hobart, Australia, Proceedings of Spatial Sciences Institute International Biennial Conference.

Liu, C. L. & Chen, Y. Q., 2009. Application of geographic information system in hydrological models: A review. In: *From headwaters to the ocean: Hydrological change and water management.* London: Taylor & Francis Group, pp. 217-222.

Li, Z., Q. Zhu and C. Gold (2005), Digital Terrain Modeling: Principles and Methodology, *CRC Press,* Boca Raton, London, New York, and Washington, D.C.

Li, Z., 2014. Watershed modeling using arc hydro based on DEMs: a case study in Jackpine watershed. *Environmental Systems Research,* 3(11).

Maidment, D. R., 2004. Arc Hydro Data Model: A Hydrologic Data Integration Tool. *Southwest Hydrology,* pp. 18-19.

Martz, L. & Garbrecht, J., 1993. Automated extraction of drainage network and watershed data from digital elevation models. *Water Resource Bulletin,* 39(6), pp. 901-908.

MSB (2014). *Kartläggning av skyfalls påverkan på samhälls- viktig verksamhet*.

O'Callaghan, J. & Mark, D., 1984. The extraction of drainage networks from digital elevation data. *Computer vision, graphics, and image processing. 28 (3),,* 28(3), pp. 323-344.

Pan, F., Stieglitz, M. & McKane, R. B., 2012. An algorithm for treating flat areas and depressions in digital elevation models using linear interpolation. *Water Resources Research,* Volume 48.

Pilesjö, P. & Hasan, A., 2014. A Triangular form based multiple flow algorithm to estimate overland flow distribution and accumulation on a Digital Elevation Model. *Transactions in GIS,* 18(1), pp. 108-124.

Pourali, S., Arrowsmith, C., Mitchell, D. & Matkan, A., 2014. Modelling An Overland Water Flow Path In An Urban Catchment Using GIS. *Geoinformatica: An International Journal (GIIJ),* 4(1).

Soille, P., 2004. Optimal removal of spurious pits in grid digital elevation models. *Water Resources Research,* Volume 40.

Sorooshian, S., Hsu, K.L., Coppola, E., Tomassetti, B., Verdecchia, M., Visconti, G. (Eds.), 2008. *Hydrological Modelling and the Water Cycle: Coupling the Atmospheric and Hydrological Models*. Springer-Verlag Berlin Heidelberg.

Sui, D. & Maggio, R. C., 1999. Integrating GIS with hydrological modeling: practices, problems, and prospects. *Computers, Environment and Urban Systems,* Volume 23, pp. 33-51.

Tarboton, D. G. & Ames, D. P., 2001. *Advances in the mapping of flow networks from digital elevation data.* Orlando, Florida, s.n.

T.M Klok, 2012. Modelling of Stormwater Overland Flow in Urban Areas. *Tauw*, pp 37-38.

Urías, H. Q., Garcia, H. & Plata Mendoza, J. S., 2007. Determination of the Relationship Between Precipitation and Return Periods to Assess Flood Risks in the City of Juarez, Mexico. *Proceedings of the Southern Illinois University Carbondale UCOWR conference,* Issue Paper 47.

VA Syd, 2012. *Åtgärdsplan för Lunds avlopp* (Action Plan for Lund sewage)

Zandbergen, P. A., 2006. The effect of cell resolution on depressions in Digital Elevation Models. *Applied GIS,* 2(1), pp. 04.1-04.35.

Zhou, Q., Pilesjö, P. & Chen, Y., 2011. Estimating surface flow paths on a digital elevation model using a triangular facet network. *Water Resources Research,* Volume 47.

Institutionen för naturgeografi och ekosystemvetenskap, Lunds Universitet.

Studentexamensarbete (seminarieuppsatser). Uppsatserna finns tillgängliga på institutionens geobibliotek, Sölvegatan 12, 223 62 LUND. Serien startade 1985. Hela listan och själva uppsatserna är även tillgängliga på LUP student papers (https://lup.lub.lu.se/student-papers/search/) och via Geobiblioteket (www.geobib.lu.se)

The student thesis reports are available at the Geo-Library, Department of Physical Geography and Ecosystem Science, University of Lund, Sölvegatan 12, S-223 62 Lund, Sweden. Report series started 1985. The complete list and electronic versions are also electronic available at the LUP student papers (https://lup.lub.lu.se/student-papers/search/) and through the Geo-library (www.geobib.lu.se)

400 Sofia Sjögren (2016) Effective methods for prediction and visualization of contaminated soil volumes in 3D with GIS

401 Jayan Wijesingha (2016) Geometric quality assessment of multi-rotor unmanned aerial vehicle-borne remote sensing products for precision agriculture

402 Jenny Ahlstrand (2016) Effects of altered precipitation regimes on bryophyte carbon dynamics in a Peruvian tropical montane cloud forest

403 Peter Markus (2016) Design and development of a prototype mobile geographical information system for real-time collection and storage of traffic accident data

404 Christos Bountzouklis (2016) Monitoring of Santorini (Greece) volcano during post-unrest period (2014-2016) with interferometric time series of Sentinel-1A

405 Gea Hallen (2016) Porous asphalt as a method for reducing urban storm water runoff in Lund, Sweden

406 Marcus Rudolf (2016) Spatiotemporal reconstructions of black carbon, organic matter and heavy metals in coastal records of south-west Sweden

407 Sophie Rudbäck (2016) The spatial growth pattern and directional properties of *Dryas octopetala* on Spitsbergen, Svalbard

408 Julia Schütt (2017) Assessment of forcing mechanisms on net community production and dissolved inorganic carbon dynamics in the Southern Ocean using glider data

409 Abdalla Eltayeb A. Mohamed (2016) Mapping tree canopy cover in the semi-arid Sahel using satellite remote sensing and Google Earth imagery

410 Ying Zhou (2016) The link between secondary organic aerosol and monoterpenes at a boreal forest site

411 Matthew Corney (2016) Preparation and analysis of crowdsourced GPS bicycling data: a study of Skåne, Sweden

412 Louise Hannon Bradshaw (2017) Sweden, forests & wind storms: Developing a model to predict storm damage to forests in Kronoberg county

413 Joel D. White (2017) Shifts within the carbon cycle in response to the absence of keystone herbivore *Ovibos moschatus* in a high arctic mire

414 Kristofer Karlsson (2017) Greenhouse gas flux at a temperate peatland: a comparison of the eddy covariance method and the flux-gradient method

415 Md. Monirul Islam (2017) Tracing mangrove forest dynamics of Bangladesh using historical Landsat data

416 Bos Brendan Bos (2017) The effects of tropical cyclones on the carbon cycle

417 Martynas Cerniauskas (2017) Estimating wildfire-attributed boreal forest burn in Central and Eastern Siberia during summer of 2016

418 Caroline Hall (2017)The mass balance and equilibrium line altitude trends of glaciers in northern Sweden

419 Clara Kjällman (2017) Changing landscapes: Wetlands in the Swedish municipality Helsingborg 1820-2016

420 Raluca Munteanu (2017) The effects of changing temperature and precipitation rates on free-living soil Nematoda in Norway.

421 Neija Maegaard Elvekjær (2017) Assessing Land degradation in global drylands and possible linkages to socio-economic inequality

422 Petra Oberhollenzer, (2017) Reforestation of Alpine Grasslands in South Tyrol: Assessing spatial changes based on LANDSAT data 1986-2016

423 Femke, Pijcke (2017) Change of water surface area in northern Sweden

424 Alexandra Pongracz (2017) Modelling global Gross Primary Production using the correlation between key leaf traits

425 Marie Skogseid (2017) Climate Change in Kenya - A review of literature and evaluation of temperature and precipitation data

426 Ida Pettersson (2017) Ekologisk kompensation och habitatbanker i kommunalt planarbete

427 Denice Adlerklint (2017) Climate Change Adaptation Strategies for Urban Stormwater Management – A comparative study of municipalities in Scania

428 Johanna Andersson (2017) Using geographically weighted regression (GWR) to explore spatial variations in the relationship between public transport accessibility and car use : a case study in Lund and Malmö, Sweden

429 Elisabeth Farrington (2017) Investigating the spatial patterns and climate dependency of Tick-Borne Encephalitis in Sweden

430 David Mårtensson (2017) Modeling habitats for vascular plants using climate factors and scenarios - Decreasing presence probability for red listed plants in Scania

431 Maja Jensen (2017) Hydrology and surface water chemistry in a small forested catchment : which factors influence surface water acidity?

432 Iris Behrens (2017) Watershed delineation for runoff estimations to culverts in the Swedish road network : a comparison between two GIS based hydrological modelling methods and a manually delineated watershed

433 Jenny Hansson (2017) Identifying large-scale land acquisitions and their agro-ecological consequences : a remote sensing based study in Ghana

434 Linn Gardell (2017) Skyddande, bevarande och skapande av urbana ekosystemtjänster i svenska kommuner

435 Johanna Andersson (2017) Utvärdering av modellerad solinstrålning i södra Sverige med Points Solar Radiation i ArcGIS

436 Huiting Huang (2017) Estimating area of vector polygons on spherical and ellipsoidal earth models with application in estimating regional carbon flows

437 Leif Holmquist (2017) Spatial runner: environmental and musical exposure effects on runners through an idealized routing network

438 Adriana Bota (2017) Methodology for creating historical land use databases – a case study for ICOS-station Hyltemossa, Sweden

439 Michael Araya Ghebremariam (2017) Urban flood modelling: a GIS based approach in Lomma, Skåne region